Surface Runoff

Yanhong Guo, Yinsheng Zhang, Teng Zhang, Kunxin Wang, Jie Ding, and Haifeng Gao

Contents

Y. Guo · T. Zhang · K. Wang · J. Ding · H. Gao
Key Laboratory of Tibetan Environment Changes and Land Surface Processes, Institute of Tibetan Plateau Research, Chinese Academy of Sciences, Beijing, China

Y. Zhang (✉)
Key Laboratory of Tibetan Environment Changes and Land Surface Processes, Institute of Tibetan Plateau Research, Chinese Academy of Sciences, Beijing, China

CAS Center for Excellence in Tibetan Plateau Earth Sciences, Beijing, China
e-mail: yszhang@itpcas.ac.cn

X. Li, H. Vereecken (eds.), *Observation and Measurement of Ecohydrological Processes*, Ecohydrology, https://doi.org/10.1007/978-3-662-48297-1_8

Abstract

Surface runoff, or overland flow, is a fundamental process of interest in hydrology. Surface runoff generation can occur at multiple scales, ranging from small pools of excess water that propagate downhill to stream networks that drain large catchments. Accurate quantification of runoff is vital to clarify the mechanisms and effects of overland flow and also indispensable to understand fundamental hydrological processes. In this chapter, four kinds of measurement techniques, including runoff plot method, curve number method, isotopic tracer method, and salt solution method, are introduced. Runoff plot experiments are often conducted to evaluate the rainfall–runoff processes and widely used to study runoff and/or sediment losses. The curve number method is used to estimate watershed direct-runoff volume by a curve number value which is developed based on measured watershed runoff and rainfall data. The isotopic tracer method is used to measure the surface runoff by separating its contribution from multicomponent based on the mass balance of stable isotopes. The salt solution method is usually used to measure the shallow water flow by detecting the movement of salt. Besides, models of surface runoff are also summarized in this chapter. The models can be classified into conceptual models and process-based models. The conceptual models are simple transfer functions describing a linear relationship between rainfall and surface runoff. While the process-based models take into account of the spatial variability of climate, soil, vegetation, and terrain, which are able to make a series of hydrological processes interconnected. Despite their complexities, the process-based models are very helpful to study the changes in hydrological processes caused by human activities. Furthermore, the vegetation has important impact on surface runoff. For instance, with the increase of vegetation coverage, surface runoff can be reduced effectively. And root induces macropores, which are of importance for runoff mitigation due to their large diameters and high connectivity, enhancing rapid rainfall infiltration and percolation to deeper soil layers. Finally, we put forward some challenges about the measurement and simulation of the surface runoff including the establishment of surface runoff observation network in different ecological system, the combination of land surface model and distributed hydrological model, and the coupling between ecological processes and the runoff process on different scales.

Keywords
Surface runoff · Runoff observation techniques · Runoff modeling · Vegetation · Root impact

Introduction

Surface Runoff Definition

The flow of a water layer over the surface and through the pores of soils and sediments that is coming out of the watershed is termed as a runoff. There are three components of the runoff from watersheds (Dingman 2002; Rumynin 2015): (i) surface runoff or overland flow (sometimes termed as direct runoff), (ii) subsurface runoff or interflow (throughflow), and (iii) groundwater runoff or baseflow (Fig. 1). The surface runoff is a two-dimensional flow occurring on slopes or in ephemeral drainage patterns. Different mechanisms involved in runoff generation are discussed below. Surface runoff rapidly reaches the nearest discharge zones, thus showing a quick response to a rain event and/or snow melting.

Surface Runoff Formation Mechanisms

The development of the basis for quantifying the transformation of rainfall to runoff has been a prime target of hydrologists for several generations. In general, two forms of runoff generation are widely accepted (Rumynin 2015): (i) the infiltration excess

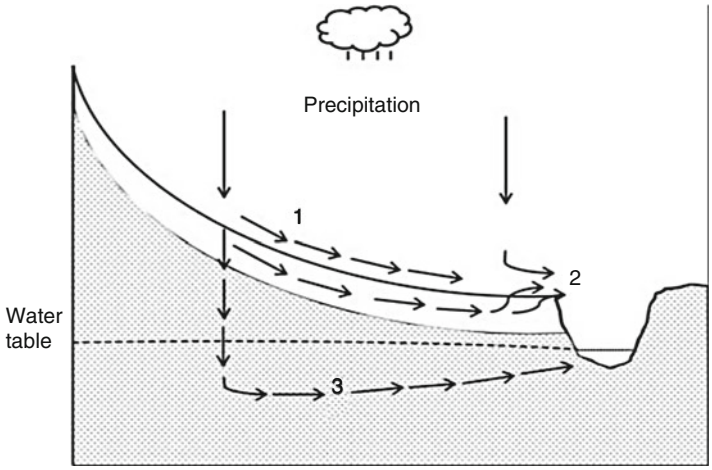

Fig. 1 Possible paths of water moving downhill: path 1 is Horton overland flow, path 2 is saturation overland flow, path 3 is groundwater flow. The unshaded zone indicates highly permeable topsoil, and the shaded zone represents less permeable subsoil

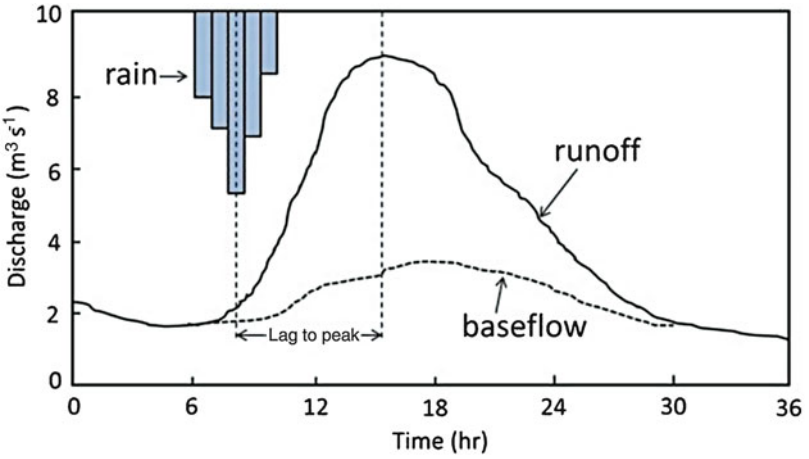

Fig. 2 A conceptual illustration of the runoff evolution due to precipitation

runoff (Horton overland flow) and (ii) the saturation excess runoff (Dunne or saturation overland flow) (Fig. 2).

Infiltration Excess Runoff

The classical model of surface runoff generation (Fig. 3) is by an infiltration excess mechanism in which rainfall intensity exceeds the local infiltration capacity of the soil for a sufficient period for any depression storage. In this way, the downslope flow is initiated at the soil surface. This will not occur where the permeability of the soil is high in comparison with expected rainfall intensities. This is not for the case that all the rainfall infiltrates before bringing the surface to saturation (the time to ponding). Such a basis of the infiltration excess was formulated in the 1930s by Robert Horton (Horton et al. 1940). It should be mentioned that the infiltration here is considered independent of overland flow dynamics resulting in weak coupling of the two processes. Horton overland flow is rare in vegetated humid region. It is common in areas devoid of vegetation such as semiarid rangelands and compacted soil. The concept in such a formation mechanism is soil infiltration capacity, $f = f(t)$, implying the maximal rate at which rainwater can be adsorbed by soil under given conditions, function f is potential infiltration.

Due to nonlinearity of flow in unsaturated soil, f decreases continuously throughout the rainfall period, and thus it behaves similar to the decay function. All rain water may go into the soil when the precipitation (p) is less than the potential infiltration. When p is greater than f, the water accumulation on the ground surface will be $q = p - f$, representing the potential of the process of water flow over the surface.

$$i\,(t) = min[p(t), f\,(t)] \tag{1}$$

where $i(t)$ is the actual rate of infiltration. The quantitative description of the process implies determining the moment t_i when the infiltration capacity f equals p. At this

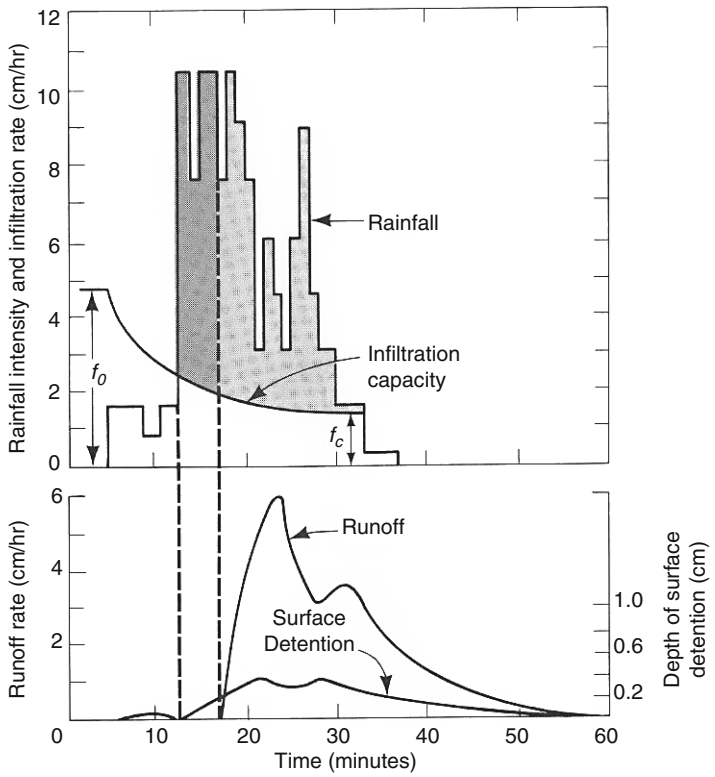

Fig. 3 Schematic chart of infiltration-excess runoff formation

time, the soil moisture reaches to its maximum value nearly equal to the soil porosity. Subsequently, $f = f(t-t_i)$ becomes less than p, resulting in surface runoff. Because the precipitation rate exceeds the infiltration capacity, there is excess precipitation available for surface runoff,

$$q(t) = \begin{cases} 0, & 0 < t < t_i \\ p - f(t - t_i), & t > t_i \end{cases} \tag{2}$$

$q(t)$ is the infiltration excess runoff rate (or intensity). Mathematically, the ponding time, t_i, is the moment when the flux boundary condition changes to a head boundary condition.

Saturation Excess Runoff

Interestingly, the surface runoff can occur in land surface with high permeability in the regions where the precipitation is always less than the infiltration capacity. This is especially true in the humid region of which groundwater table is high and the soils and vadose zone rocks are heterogeneous. Such a phenomenon is usually referred to

saturation excess runoff. This formation uses the Dunne assumption that all precipitation enters the soil and runoff occurs due to the inability of soil to absorb any more water (Dunne 1978; Dunne et al. 1975). They reflect the limited ability of soil and underlying rocks to accumulate water, for example, in areas where a thin soil layer is underlain by low-permeability deposits or in areas with shallow groundwater table. When falling onto such areas, precipitation has no storage reserve, it will directly transform into surface runoff. Therefore, the Dunne overland flow generation is controlled, along with soil hydraulic properties, by two major factors including the geomorphology (e.g., the shape and the slope) of the catchment and its subsurface hydrology (Willgoose and Perera 2001).

The saturation excess runoff in humid regions with coarse-texture soils is generated by saturation from below or by a rising groundwater table or by discharging sporadic horizontal flow of water (through flow) within the soil layer. Many studies have shown that overland flow in areas with humid climate form within relatively small areas (as compared with the total watershed area) with higher water table. This commonly occur in hill slopes, river valleys, and swales. Such saturated areas, where saturation excess runoff is produced, are referred as variable source areas (VSAs). The reason is that these areas are limited to the close vicinity of the stream, but they can expand during the storm resulting in larger rates of runoff generation. Previous studies showed that up to two-thirds of direct runoff can originate from the VSAs occupying only 5–20% of the watershed area (Boughton 1993; Ogden and Watts 2000). In general, the peak rate of saturation excess runoff varies, but it is less than that of infiltration excess runoff, because only a portion of the drainage basin is contributing saturation overland flow. Flow velocity of the former is somewhat smaller than that of infiltration excess runoff, because saturation overland flow takes place on gentle vegetated surface.

General Observational Techniques of Surface Runoff

Runoff Plot Measurement

Surface runoff, or overland flow, is a fundamental process of interest in hydrology. Surface runoff generation can occur at multiple scales, ranging from small pools of excess water that propagate downhill to stream networks that drain large catchments. Accurate measurement of runoff quantity is vital to clarify the mechanisms and effects of overland flow and also indispensable to understand fundamental hydrological processes. As a prerequisite of watershed scale investigations, plot-scale studies are often conducted to evaluate the rainfall–runoff processes with better control over the controlling, under which circumstances, runoff plot experiments were used widely to study runoff and/or sediment losses from different field sites around the world (Negi et al. 1998; Sarkar and Dutta 2011; Sarkar et al. 2008; Singh et al. 1983). Most of the experimental set-ups used either rainfall simulators or inflow–outflow methods for evaluation of plot-scale hydrologic responses, which are also prerequisites to developing any regional hydrological model.

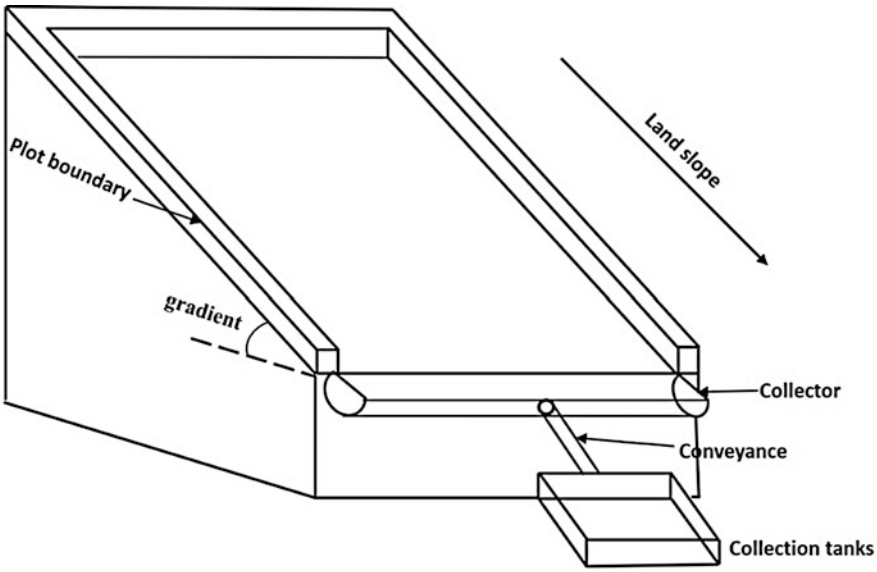

Fig. 4 Typical design of simple runoff plot layout

Outlined in general, following equipments are needed for a typical runoff plot (Mutchler 1963) (See in Fig. 4).

1. Boundaries around the plot to define the measured area.
2. Collect channel to catch and concentrate runoff from the plot.
3. Conveyance equipment to carry runoff to a collection tank.
4. Collection tanks to hold aliquot portions of runoff.

Other equipment is sometimes desired. It is helpful in analysis to have a runoff hydrograph. Hence, a rate-measuring flume can be placed between the collector unit and the sampling unit. Special heating equipment is needed if snow-melt runoff is evaluated. Principles of the key components equipped with the runoff plot can be explained in details as follows.

Plot Boundaries

As a general rule, runoff plots with planar surfaces off large stones, steep slope, or sag encourage the flow to occur. Plot area influences the amount of runoff that needs to be collected, stored, and measured after a rainfall event or series of rainfall events (Zhang et al. 2015). Several methods have been used to define runoff plot areas. Dikes in combination with terrace channels have been used generally on plots larger than one-fourth acre. Strips of 16-gage galvanized steel approximately 9 inches high by 6- to 12-feet long, with corrugations running across the small dimension, make

excellent boundaries for cultivated plots. These are comparatively easy to install and maintain. Where the boundaries are permanently installed, smooth galvanized steel strips, 14-gage are preferred.

Runoff Collector

Collecting equipment of many different designs and materials has been used on the runoff stations around the world. The collector generally acts as a weir across the bottom of the plot and a channel for runoff to the sampling unit. Sheet-metal construction is preferred to concrete, because the collector elevation must be adjusted to the level of the plot as erosion occurs. An endplate made of heavy gage galvanized steel blocks off the plot end and furnishes a stable attachment for the trough of the collector. The endplate should extend at least 8 inches below the collector trough.

The collector trough acts as a channel for the runoff material. This trough (together with the endplate) is designed to reach across the entire width of narrow plots. For plots wider than 14 feet, it is best to concentrate the runoff before collecting it.

The major elements of collector trough design are depth, width, and bottom slope. Design depth can be figured two ways, depending on whether a measure flume is used or whether runoff is conducted directly to the sludge tank. If a flume is used, depth of the collector is controlled by the size of the approach channel required by the flume. In other words, the design is started by choosing the type and size flume necessary to handle maximum runoff. Thus, depth of the collector is equal to depth of the flume plus about 10% freeboard.

When only a conveyance pipe is used (no rate measurement), the collector depth is based on the pipe size needed to carry the runoff load. After the collector depth is calculated as discussed above, a freeboard of approximately 0.4 foot is added to the collector trough. This freeboard is needed primarily to form a notch across the plot end and may be changed to suit local design requirements.

Figure 5a shows an example. Although the design worked appropriately during many storms, it did not work in some other cases. Replacement by a design that concentrated flows vertically and produced supercritical flow in the channel leading to collection tanks (Fig. 5b, c) overcame the problem. However, there are a number of designs where flows are forced to concentrate on the eroding area so that they produce results that are open to question (Kinnell 2016).

Figure 6a shows an example where flow was forced to concentrate on the eroding surface and sedimentation occurred on the plot just upslope of a flume. The kite-shaped plot shown in Figure 5.1.1 in Kuhn et al. (2014) provides another example where flows are forced to concentrate on the eroding surface. Figure 6b shows schematics of other designs that have been used in experiments reported in literature (Strohmeier et al. 2016; Vaezi et al. 2008; Zhang et al. 2015) but produce results that are open to question. Ensuring that surface water flows freely over the whole of the eroding surface is essential in all rainfall erosion experiments no matter what the scale or whether the experiments are done in the field or in the laboratory.

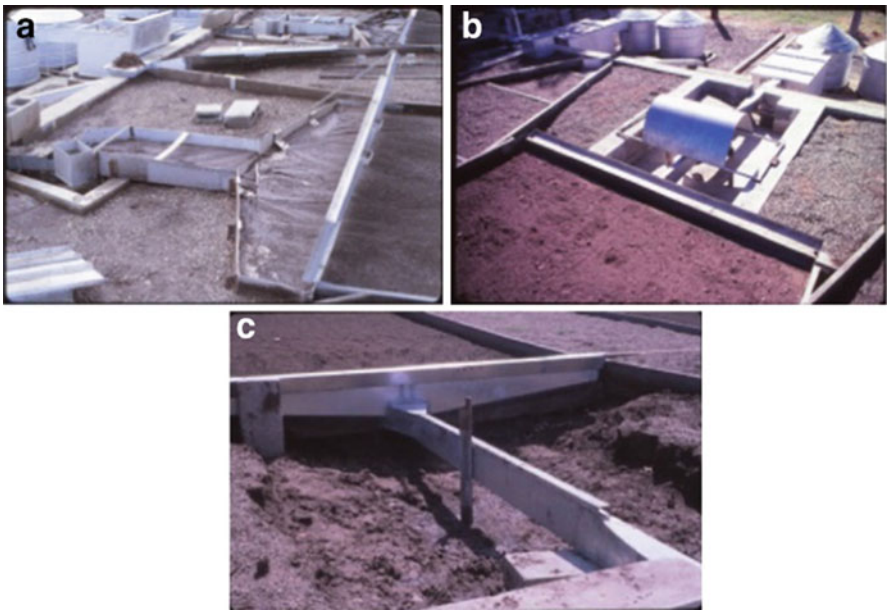

Fig. 5 Runoff collection equipment with 40 m long 2.6 m wide bare fallow plots at Gunnedah, New South Wales, Australia: (**a**) shows the design commonly used by the then Soil Conservation Service of New South Wales and (**b**) and (**c**) show the design that replaced it (Kinnell 2016)

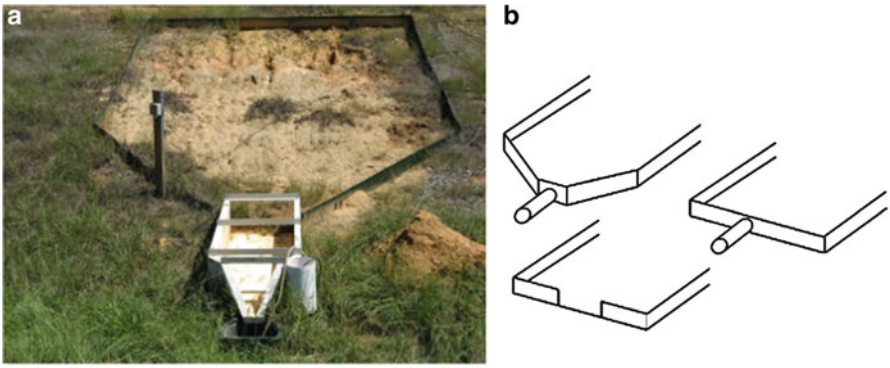

Fig. 6 Examples of designs of runoff collection systems that should not be used on runoff and soil loss plots (Kinnell 2016)

Collection Tanks

Tanks are used to store all the sludge and the aliquot of the soil loss-runoff mixture. Oval end stock water tanks make good sludge tanks and are commercially available in 2-foot height. Usually 1 mm of runoff on a square meter of plot will result in 1 L of water for collection and storage so that the runoff collection system should not overflow between the end of the plot and tanks designed to collect runoff (Kinnell

2016). Hence, the storage system should be made of inexpensive mild sheet steel, painted against rust and be tailored to the runoff producing capacity of the plots in the climate at the location being studied (Kinnell 2016). Some companies will make tanks 29 or 30 inches high on special order, which are preferable to a 2-foot height because of the higher storage capacity. Round tanks are recommended for aliquot storage; these usually have to be custom made.

The sludge tank unit has two major functions: (i) To retain all the heavy soil material and pass only a suspended sediment mixture to the divisor unit and (ii) to store sludge which will make up the bulk of the soil loss from the runoff plot. Turbulence in the sludge tank due to high entrance velocities from the runoff plot is reduced by placing two screens across the flow through the sludge tank, thus increasing deposition. The screens also keep trash from clogging up the divisor. The screens do not extend to the tank bottom and freeboard is allowed at the top. This is done to insure flow even though the screens become filled with trash. Floor space between the tank inlet and first screen is left for a can to catch low flows, so that the entire tank need not be cleaned after every rain shower. The 50-ton-per-acre maximum soil loss figure discussed under design criteria is used to calculate storage capacity of the sludge tank. A cubic foot of soil weighs from 60 to 100 pounds.

As plot size increases, the ability to store all runoff and soil loss becomes increasingly difficult. In some cases, a series of connected tanks is installed with the overflow from one tank feeding to another being subsampled by devices called multislot divisors. Outflow from the tank flows through a number of slots with only one being used to pass a known portion of the outflow to the next tank (Pinson et al. 2004). Deposition of coarse sediment usually takes place in the first tank so that the flow into the downstream tank usually contains only fine suspended load. Cascading to additional tanks with the outflows passing through multislot divisors provides the means of storing information on runoff and soil loss for large runoff events that would be impossible to obtain otherwise. The separation of coarse and fine loads also enables the runoff in the downstream tanks to be mixed and subsampled to obtain sediment concentrations that can be used to determine the sediment load in the tanks. However, in the first tank, that cannot be done, because the fast settling nature of the coarse sediment results in underestimation of the sediment concentration (Ciesiolka et al. 2006). Consequently, the most accurate method involves collecting the coarse sediment from the water in the first tank to enable it to be dried and weighed separately. The fine material in the water from the first tank can then be determined through subsampling the liquid once the coarse material has been removed. This approach was adopted by Kinnell (1983) who ensured that subsamples were taken while stirring the mixture after removal of coarse material. This resulted in variations in pairs of subsamples about their mean being frequently within $\pm 1\%$ and seldom exceeding $\pm 3\%$.

Apart from multislot devisors, some other devices have been developed to reduce the quantities of runoff and soil loss that have to be stored during one or more erosion events. With the Coshocton Wheel sampler (Brakensiek et al. 1979; Carter and Parsons 1967), flow from the runoff collector rotates a slot through the outflow collector with the speed of rotation controlled by flow falling on to vanes (Fig. 7a).

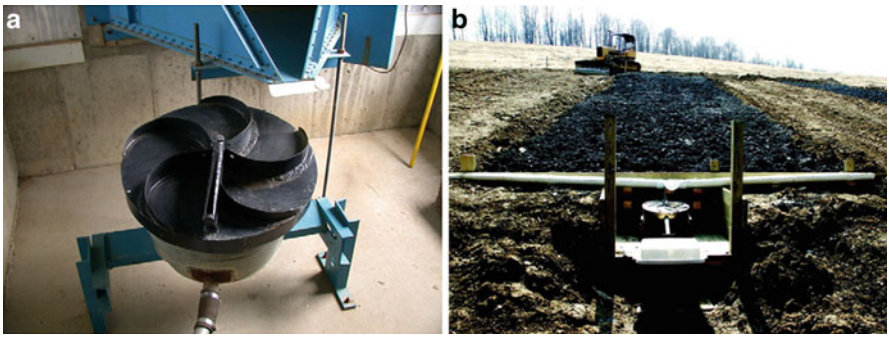

Fig. 7 (**a**) An early version of the Coshocton Wheel used by the USDA-ARS. (**b**) An example of a Coshocton Wheel installed on a plot to measure runoff and soil loss (Kinnell 2016)

Runoff measuring devices like H-flumes can cause deposition to occur upslope of Coshocton Wheels and care needs to be taken to ensure that such devices do not cause ponding and deposition on the eroding surface such as shown in Fig. 7a. A H-flume–Coshocton Wheel system (see Fig. 2 in Mutchler et al. (1988)) was used in the evaluation of the product of runoff rate and rain kinetic energy flux as an alternative to the EI30 index at Holly Springs, MS, USA (Kinnell 1995; Kinnell et al. 1994). Coarse material deposited upslope of the flume was measured separately from the material collected by the Coshocton Wheel.

Another approach to measuring runoff centers about the use of the tipping bucket method to measure runoff (Nehls et al. 2011; Yu et al. 1997; Zhao et al. 2001). Tipping buckets were initially developed as a meteorological device for measuring rainfall but have been expanded in size to measure runoff (Edwards et al. 1974; Khan and Ong 1997; Pillsbury et al. 1962). Sediment sampling is achieved in some cases by using slots to collect runoff and sediment as the bucket empties (Deasy et al. 2009; Silgram et al. 2010). Some designs are better suited to situations where only fine material is discharged with runoff.

As an example, in Fig. 8, runoff water was collected and quantified at the lower end of each plot throughout the growing season using a tipping-bucket runoff metering apparatus (Fig. 8). Buckets were calibrated (one tip represents 3 L of runoff) and maintained to provide precise measure of amount of runoff per tip. Numbers of tips were counted using mechanical runoff counters. Collection of samples in 3.79 L borosilicate glass bottles was carried out through a flow-restricted composite collection system (approximately 40 ml per tip was collected) (Antonious 2015).

Experiments Using Artificial Rainfall

Comprehensively speaking, a number of instruments have been used to quantify runoff. The most basic measurement method involves diverting flow to a barrel or similar structure (Dosskey et al. 2007; Hudson 1993; Meals and Braun 2006). Water quantity, chemistry, and sediment measurements can then be taken on the collected water. However, for specific application, designs of runoff plot varied according to the local climate and other conditions and can be conducted under two

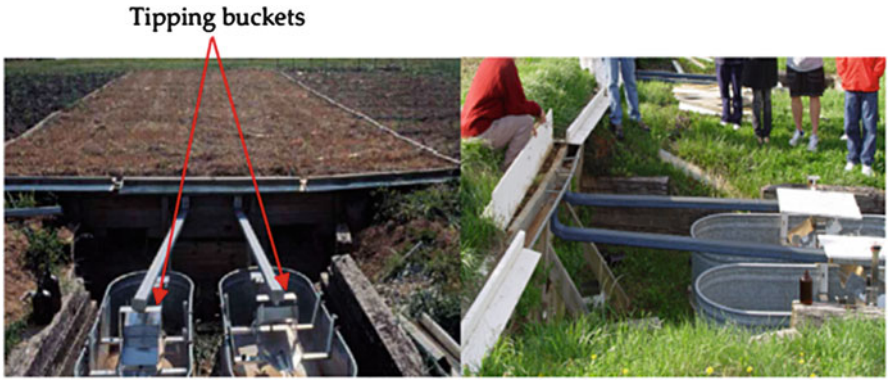

Fig. 8 Surface runoff water collection using tipping buckets installed down the field slope. A gutter was installed across the lower end of each plot with 5% slope to direct runoff to the tipping buckets and collection bottles for runoff (Antonious 2015)

circumstances: in-situ measurement without any artificial water pumping as the above introduction and experiment simulations with water input by rainfall simulators or other sources. Below are several runoff plot examples applicable to different circumstances. Experiments using runoff plots under natural rainfall such as those used to develop the Universal Soil Loss Equation are still undertaken from time to time in various parts of the world but, as noted earlier, the USDA-Purdue rainfall simulator, or "rainulator," was developed by Meyer and McCune (1958) as a tool to conduct experiments to supplement the USLE natural rainfall database. Wischmeier and Mannering (1969) used the rainulator on 55 soils to examine the relationship of soil properties to erodibility. Each test consisted of three storms. The first was for 60 min on an initially dry soil. The second storm applied the next day was applied under what was considered to be a wet condition, and that was then followed by another storm on the same day on a surface that was considered to be in very wet condition. The different values of erodibility recorded for the different antecedent moisture conditions were then used in an equation that calculated the K for the climate in central USA (Romkens 1985).

There are many different rainfall simulator designs using a wide variety of nozzles reported in the literature (Iserloh et al. 2013a; Meyer 1994). The rainfall simulators that have been the development of WEPP and RHEM have used TeeJet 2HH-SS50WSQ nozzles. In WEPP interrill erosion model given in Flanagan et al. (Flanagan and Nearing 1995), there is a term (Fnozzle) to take account of the use of other nozzles. That provision is not documented well in many other places and consequently, the data on interrill erodibilities published without taking account of differences between the nozzles used and TeeJet 2HH-SS50WSQ nozzles (Mahmoodabadi and Cerdà 2013; Romero et al. 2007). Apart from Iserloh et al. (2013b), there appears to be little or no work reported on the effect of different rainfall simulators on sediment discharged from interrill areas. Figure 9 shows the

Fig. 9 The artificial simulated rainfall device (Mayerhofer et al. 2017)

artificial simulated rainfall device used in studying the effects of land use and land cover on surface runoff in the catchment area of the Alps.

Runoff Measurement by Curve Number (CN) Method

Theory

Runoff estimates are often needed for ungauged watersheds for engineering design of hydraulic structures, watershed the U.S. Department of Agriculture (USDA) – Soil Conservation Service (SCS) developed a method for estimating rainfed runoff volume based on measured total rainfall and direct runoff, and physical watershed features. This method is simple to use and requires basic descriptive inputs that are converted to numeric values for estimation of watershed direct-runoff volume. The curve number (CN) method is widely used by engineers and hydrologists as a simple watershed model, and as the runoff-estimating component in more complex, watershed models. The method depends on using measured watershed runoff and rainfall data to develop a CN value that reflects the CN value that should be developed from measured data.

The maximum potential retention (S) can be calculated from the CN value which is able to be determined in considering hydrological, soil property, land use and surface conditions, and soil moisture content before runoff occurs (Mishra and Singh 2013). However, the CN method does not consider rainfall intensity, and there are questions as to whether it is applicable for areas outside of the USA (Yamashita et al. 2006).

On the other hand, Chong and Green (1983) introduced the following Eq. (1) which combining with the SCS rainfall-runoff equation and the maximum potential

retention (S) of a watershed in order to estimate the value of sorptivity. This equation shows that it is possible to estimate the volume of rainfall runoff from a watershed, if there is a relationship between sorptivity values and initial soil moisture contents

$$S = \frac{1}{2} R_i^{-1/2} K_{Sat}^{-1/2} [Sp(\theta)]^2 \tag{3}$$

where S is the maximum potential retention. $Sp(\theta)$ is soil sorptivity, K_{sat} is saturated soil hydraulic conductivity, and R_i: rainfall intensity. The term "sorptivity" was introduced by Philip (1957a) in his well-known two-term infiltration equation. As described by Philip, sorptivity, $Sp(\theta)$, is a measure of the uptake of water by soil without gravitational effects. According to the Philip two-term equation, this coefficient is one of the most important soil parameters governing the early portion of infiltration.

Thus the relationship between sorptivity values and soil moisture contents and estimated the maximum potential retention using Eq. (3) with rainfall intensity and saturated soil hydraulic conductivity can be clarified. Finally, the estimated surface runoff volumes for each rainfall event were calculated using sorptivity. On the other hand, surface runoff volumes using the CN method were also estimated in order to compare the surface runoff volumes.

Experiment Setup

A water reservoir to measure rainfall runoff volume from a catchment area was constructed in an experimental field with covered plastic film sheet to prevent percolation into soils. In order to measure the water level of this reservoir, a water pressure sensor with a data logger was installed at the bottom of the reservoir. At the same time, we measured the atmospheric pressure using another pressure sensor with a data logger so that we can get a water depth in the reservoir to calculate a difference value of both pressure sensors. Other meteorological data such as air temperature, relative humidity, wind speed, solar radiation, and rainfall were also collected in the experimental field (Fig. 10).

A disc tension permeameter can be fabricated in order to measure water infiltration in the soil, which is characterized by in situ saturated and unsaturated soil hydraulic properties. It is mainly used to provide estimates of sorptivity and the hydraulic conductivity of the soil near saturation. In order to clarify the relationship between sorptivity values and initial moisture contents in soils in the catchment area, we carried out an experiment using the disc tension permeameter near the catchment area located in ATRAC. The steps for measuring sorptivity are as follows.

Firstly, surface top soils of in 2–3 cm thickness are moved out and a metal cylinder of diameter 15 cm is vertically inserted into soils. The disc tension permeameter with 4 cm suction is installed on the cylinder. After starting infiltration into soils of the metal cylinder, accumulated infiltration amounts at each elapsed time are measured. Water to surface soil can also be supplied close to the cylinder in order to change soil moisture content of top soils so that sorptivity values under different soil moisture conditions could be measured.

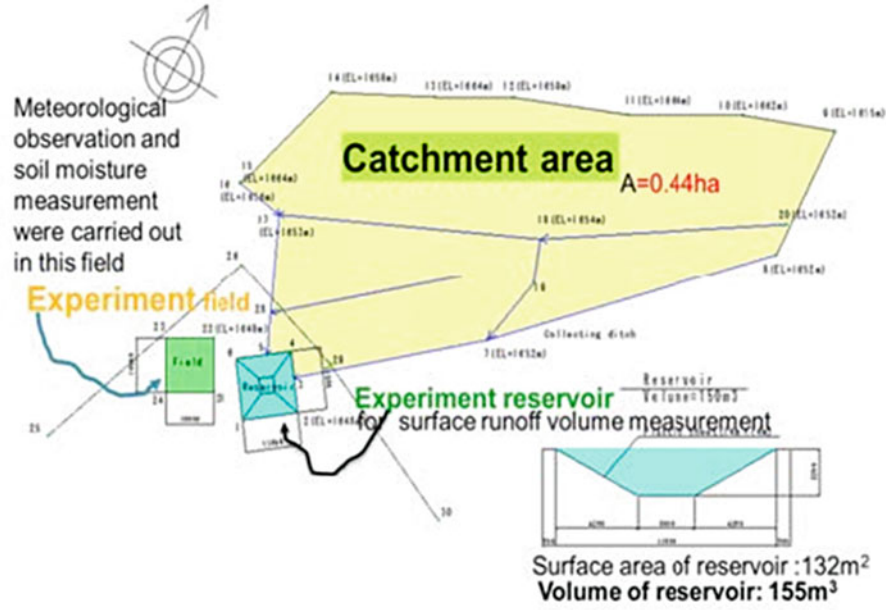

Fig. 10 Layout plan of experimental reservoir, catchment area, canals, and experiment field conducted by Watanabe et al. (2012)

Undisturbed soil cores were collected using a 100 cm^3 soil sampler to measure the moisture content of the soil surface close to the cylinder so that the relationship between sorptivity values and initial soil moisture content could be clarified for each sorptivity measurement.

Runoff Measurement by Isotopic Tracers

Theory

Hydrological responses of hillslopes are determined by a number of factors associated with parent geological material, topography, climate, and vegetation. The processes whereby rainfall becomes runoff continue to be difficult to quantify and conceptualize. Hydrograph separation with natural tracers or isotopes has become a popular method to gain comprehensive insights into runoff processes which can date back nearly 50 years (Hubert et al. 1969).

The simplest concept of hydrograph separation distinguishes between event and pre-event water. Over the hillslope, event water is water from rain that enters and flows through the system, and pre-event water is soil that is already stored in the system at the beginning of the event. If the two end-members have a distinct difference in their isotopic signature, the surface runoff hydrograph can be separated in their contributions based on a mass balance approach (Buttle 1998):

$$Q_t = Q_p + Q_e \tag{4}$$

$$C_t Q_t = C_p Q_p + C_e Q_e \tag{5}$$

$$F_p = \frac{(C_t - C_e)}{(C_p - C_e)} \tag{6}$$

where Q_t is the surface flow/streamflow; Q_p the contribution from pre-event water; Q_e the contribution of event water; C_t, C_p, and C_e are the d values of surface runoff, pre-event water, and event water, respectively; and F_p is the fraction of pre-event water in the surface runoff. Abundance of stable water isotopes is based on the isotopic ratios ($^{18}O/^{16}O$ and $^{2}H/^{1}H$).

At the initial stage, Sklash et al. (1976) and Sklash and Farvolden (1979) provided the first, clear exposition of the main underlying assumptions implicit in the technique (initially four), which were later refined and extended to five underlying assumptions (Buttle 1994; Moore 1989):

1. The isotopic content of the event and the pre-event water are significantly different.
2. The event water maintains a constant isotopic signature in space and time or any variations can be accounted for.
3. The isotopic signature of the pre-event water is constant in space and time or any variations can be accounted for.
4. Contributions from the vadose zone must be negligible, or the isotopic signature of the soil water must be similar to that of groundwater.
5. Surface storage contributes minimally to the surface runoff.

For now, it is important to note that early isotopic hydrograph separation (IHS) work also assumed that the pre-event water could be described by a single isotopic value of water in the stream prior to the event; describing in essence, a single, integrated pre-event water signal that is assumed to be representative of the entire stored water that may contribute to surface runoff (Sklash and Farvolden 1979). A number of follow-on studies to the early two-component IHS used a multi-component approach to account for additional contributing end-members. In such cases, the standard mixing Eq. (7) and (8) were extended as follows:

$$Q_t = Q_1 + Q_2 + Q_3 + \cdots + Q_n \tag{7}$$

$$C_t Q_t = C_1 Q_1 + C_2 Q_2 + C_3 Q_3 + \cdots + C_n Q_n \tag{8}$$

where Q_n is the discharge of a particular runoff component and C_n the tracer concentration of a particular runoff component. In the case of three flow components, a second tracer or a measurement of one flow component was required. Most commonly, a stable isotope tracer was combined with a geochemical tracer (Wels et al. 1991), but sometimes a second stable isotope was used (Rice and Hornberger, 1998).

In the past, several improvements and modifications of the original hydrograph separation procedure were suggested (Harris et al. 1995; Mcdonnell et al. 1990). At the initial stage, hydrograph separation method to the hillslope runoff generation were usually applied to the simple partition of pre-event and event by adding an appropriate weighting technique (Burlando 1999; Mcdonnell et al. 1990).

Drawbacks related to a simplistic use of isotopes in runoff separation studies can be avoided by applying more sophisticated experimental and modeling approaches, ideally including fully distributed process-based multidimensional numerical modeling of the relevant hydrological processes. To prevent an excessive computational cost of the numerical solution of two- (2D) or three-dimensional (3D) governing equations of the hillslope scale flow and transport processes, it is possible to decouple the essentially 3D flow into one-dimensional (1D) vertical variably saturated flow and 1D lateral saturated flow along soil-bedrock interface (Fan and Bras 1998; Hilberts et al. 2007; Troch et al. 2002). Vogel et al. (2010) applied vertical one-dimensional dual-continuum model to describe soil water dynamics and stable isotope transport in a hillslope soil. In their analysis, the oxygen isotope was used as a natural tracer to study preferential flow effects at the site of interest. In the subsequent study, lateral component of rapid shallow subsurface flow at the same site, in addition to preferential vertical movement, was considered (Dusek et al. 2012).

Experiment Setup

Taking the studies conducted by Vogel et al. (2010) as examples. The experimental hillslope site Tomsovka is situated in the small mountain catchment Uhlirska, Jizera Mountains, Czech Republic (total area 1.78 km^2, average altitude 820 m above sea level, annual precipitation exceeding 1300 mm, average annual temperature 4.7°C).

1. Isotope sampling

   The $\delta^{18}O$ values were determined in (i) precipitation collected from the rain gauge (or from snowfall and snowpack samples during winter), (ii) surface and subsurface hillslope discharge collected from the experimental trench, and (iii) soil water extracted from the selected depths by suction cups.

   During the vegetation seasons, rainwater samples were collected at daily intervals. Because each sample represents cumulative rainfall for the period between the two samplings, the measured $\delta^{18}O$ value was averaged over the respective time interval. During the winter, weekly precipitation totals were measured by a storage gauge (rain–snow standpipe). The snow depth and snow density were measured by a snow sampling tube. Both the storage gauge water and the snowpack water were sampled (synchronously and separately) to determine the ^{18}O content. The monitoring of hillslope discharge by tipping bucket flux meters was discontinued due to freezing temperatures.

   Soil water was extracted by suction cups installed at the depths of 30 and 60 cm below the soil surface. At the beginning of the soil water extraction, the air was pumped out from the probe with a hand vacuum pump until a pressure head of about −500 cm was reached. A soil water sample was then collected in 2 to 4 d, depending on the soil moisture conditions. The extraction time was adjusted so as

to obtain at least a 20 cm^3 water sample. The pressure head increase in the probe during the extraction was about 100 cm. The sampling was repeated at approximately monthly intervals over the period of interest.

The oxygen and hydrogen isotope ratios ($\delta^{18}O$ and δD) of all of the samples can be measured on a Picarro L2130-i liquid analyzer. The measured values of $\delta^{18}O$ and δD are expressed in parts as per mil (‰) of their deviations, with respect to Vienna Standard Mean Ocean Water (V-SMOW2).

2. Related factors measurement
Soil water pressure within the soil profile was measured using a set of automated tensiometers installed at three different depths below the soil surface. The discharge of shallow subsurface flow was measured by means of experimental trench. Water entering the trench was collected at the depth of about 75 cm below the soil surface into PVC pipes. The pipe discharge was measured by tipping bucket gauges, separately for two trench sections denoted as A and B (each 4 m long). The discharge rates QA and QB were measured continuously during vegetation seasons (from May to October). The hillslope length contributing to measured subsurface runoff was estimated to be about 25 m (Hrnčíř et al. 2010), although the geographic catchment divide is located approximately 130 m above the experimental trench, winding through a gently sloping plateau. The contributing hillslope length estimate was based on the comparison of hillslope discharge to the trench and observed catchment outlet discharge (assuming that hillslope subsurface flow represents a dominant part of the catchment response and is uniform across the catchment). For the modeling purposes, the hillslope microcatchments corresponding to trench sections A and B were assumed to have approximately same geometric and material properties (hillslope length, depth to bedrock, soil stratification, soil hydraulic properties, etc.).

From the point of view of the model, the ^{18}O signature in precipitation water represents an input signal, and the isotopic composition of the subsurface hillslope discharge an output signal. The model conveys our hypothesis about the processes controlling the input-output transformation. The transformation takes place in both the soil matrix and the preferential flow domains, each being characterized by different mixing patterns of “old” and “new” water (Fig. 11). The mixing is also affected by the interdomain exchange of soil water.

Runoff Measurement by Salts

Mean flow velocity (V_m) is one of the most important hydraulic variables in soil erosion modeling, since it is dependent upon flow discharge, slope gradient, topography, and surface condition (Zhang et al. 2002). It is used to calculate friction coefficient, runoff concentration time, and other hydraulic parameters such as stream power and unit stream power, which are used to simulate the processes of both detachment and sediment transport in the process-based erosion model (De Roo et al.

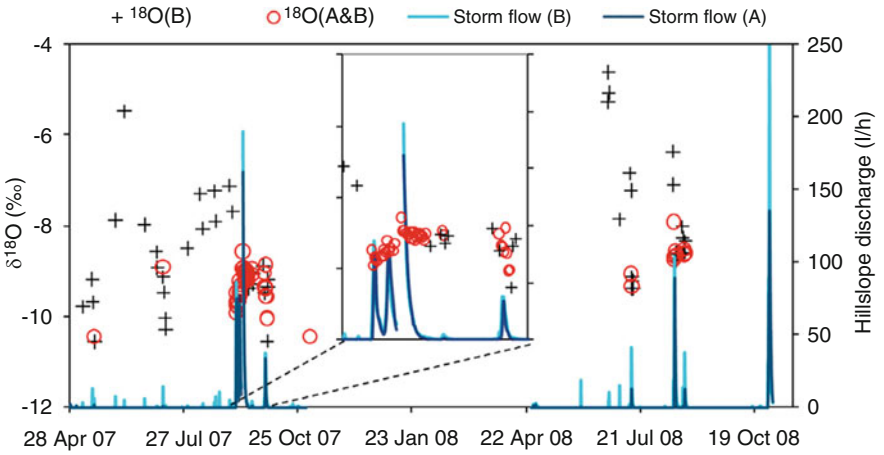

Fig. 11 Observed hillslope discharges and the corresponding ^{18}O contents. The crosses indicate the instances when only section B of the experimental trench contributed to the collected samples while no discharge was observed from section A. The circles indicate that both trench sections contributed to the samples. The period of 1 September to 4 October is enlarged to provide closer view of the major storm (the missing rising limb of the third peak is due to incomplete observation data) (Vogel et al. 2010)

2015; Zhang et al. 2010a). The measurement of shallow water flow often involves the use of a tracer. Tracers used have included dyes (Abrantes et al. 2018; Zhang et al. 2010a) and salts (electrolytes) (Planchon et al. 2005; Lei et al. 2005). Most of these methods necessarily involve the use of instrumentation to detect the tracer movement. Here we will focus on an improved method for shallow water flow velocity measurement with practical electrolyte inputs.

Theory

Salt solution in water flow is transported under influences of both convection and dispersion. Its transportation is influenced by many factors such as the flow rate, flow velocity, and the water quality. When the flow is reasonably assumed to be a one-dimensional and steady flow, its behavior is well defined and quantified by a partial differential equation (PDE).

The convectional and dispersion processes of salt a steady water flow are defined by Fick's law and the mass conservation law and is given by the differential equation for the one- D solute transport as:

$$hw\frac{\partial C}{\partial t} + hwu\frac{\partial C}{\partial x} = \frac{\partial}{\partial x}\left(hwD_H\frac{\partial C}{\partial x}\right) \tag{9}$$

where h is the depth of the water flow, m; w is the width of the flow, m; C is the electrolyte concentration, kg m^{-3}, a function of distance x and time t, proportional to the electrical conductivity of the solution; x is the coordinate down the slope, m; u is

the flow velocity, m s^{-1}; t is time, s; and D_H is the hydrodynamic dispersion coefficient, m^2 s^{-1}.

When rainfall and infiltration are ignored, the flow rate is a constant, and the velocity of the laminar flow varies little, such that:

$$Q_0 = hwu = constant \tag{10}$$

$$u = constant \tag{11}$$

which leads to

$$hw = constant \tag{12}$$

where Q_0 is the flow rate, $m^3 s^{-1}$

Combining Eq. (12) with Eq. (9) yields:

$$\frac{\partial C}{\partial t} + \frac{\partial C}{\partial x} = \frac{\partial}{\partial x}\left(hw\frac{\partial C}{\partial x}\right) \tag{13}$$

When the upper boundary condition is assumed to be a pulse, the initial and boundary conditions for Eq. (13) are given as:

$$\mathrm{C}(x,t) = C_0\delta(t) \quad x = 0 \tag{14}$$

$$\mathrm{C}(x,t) = 0 \quad x = \infty \tag{15}$$

$$\mathrm{C}(x,t) = 0 \quad t = 0 \tag{16}$$

The solution to Eq. (13) as a time-dependent function is given by (Lei et al. 2005) as:

$$\mathrm{C}(x,t) = C_0 \frac{x}{2t\sqrt{\pi D_H t}} \exp\left(-\frac{(x-ut)^2}{4D_H t}\right) \tag{17}$$

This is the analytical solution to Eq. (13), with the pulse function as the upper boundary condition. The solution quantifies the transient transport of solutes in the flowing water, under a pulse input. Equation (17) is an error function. There are three important parameters, i.e., C_0, u, and D_H to be determined to specify the functional distribution of the transient transport process.

Experiment Setup

An experimental flume of 4 m long and 15 cm wide was used to simulate the water flow, in which the solute was transported (Lei et al. 2010). The experimental system is shown in Fig. 12. The system included a computer installed with specially designed software for control of salt solute injection and sensed data logging, an interface unit, electric conductivity sensors, a salt solute injector, the flume, and the

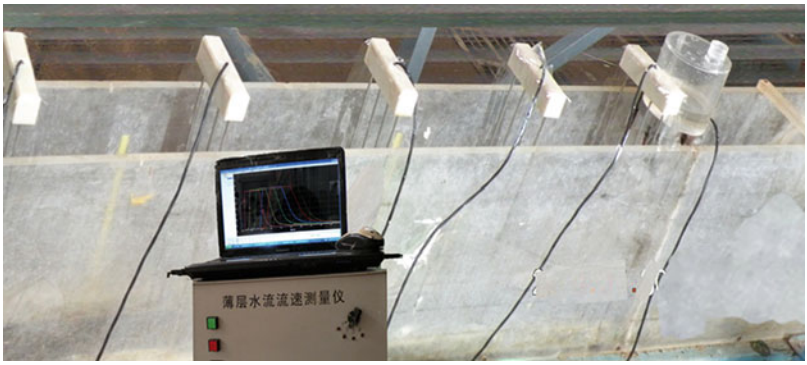

Fig. 12 Experimental equipment system (Lei et al. 2010)

water supply. The experiments involved a combination of three flow rates (Q = 12, 24, and 48 L min^{-1}) and three slope gradients (S = 4°, 8°, and 12°). The regulated water flow was introduced into the flume from the upper end. Once the flow was stabilized (within 1 min fluctuation), about 6 ml of highly saturated salt solution of KCl was injected at a location 1 m from the upper end of the flume, allowing some distance for the establishment of the steady flow.

The injection of the salt solution into the water flow was done through a computer-controlled electrical valve. The six sensors were located at 5, 30, 60, 90, 120, and 150 cm from the solute injector. The sensor 5 cm from the solution injection point was used to register the input signal. The electrical conductivity values measured at the six locations were logged into the computer through the specially designed data logger, controlled by the specially designed software.

When using this system for velocity measurement of shallow water flow in the laboratory by the method discussed above, these procedures are typically as following:

1. Wire up the system and set the flume at the required slope.
2. Place the electrical conductivity (EC) sensors at the designate locations, with one sensor located at 5 cm from the KCl solution injection point.
3. Put the prepared KCl solution into the injector container.
4. Introduce a specific water flow into the flume from its upper end, stabilize and measure it.
5. Start the software specially designed to start taking measurements.
6. The computer initiates data logging and injects salt solute into the stream via the interface unit.
7. Allow time for the solute to transport and pass through each sensor.
8. The EC values as function of time are recorded by the computer.
9. Stop data logging.
10. Run the analysis part of the software to fit the logged data from the first channel to determine the input boundary signal.

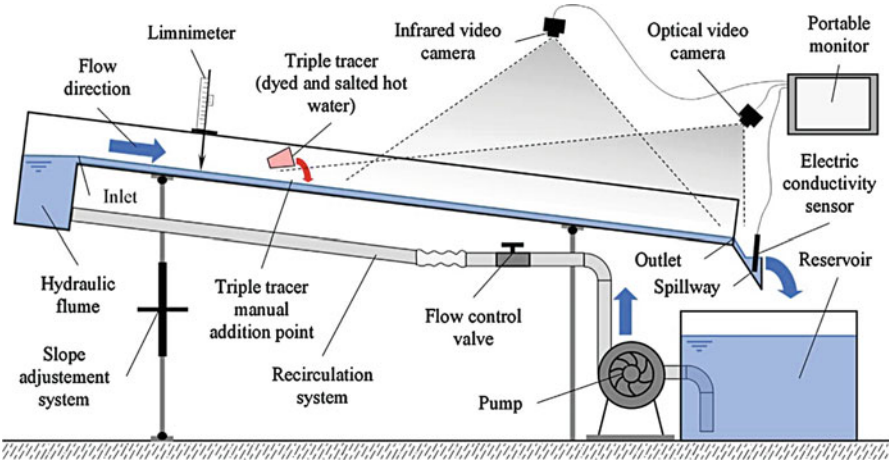

Fig. 13 Scheme (side view) of the laboratory setup used in the triple-tracer experiments (Abrantes et al. 2018)

11. Fit the logged data from the other channels with the integral equations to estimate the velocities at different locations.
12. Output the computed velocity values and other information required.

Similar experiments laboratory experiments were also conducted to compare the traditional dye and salt tracer techniques to the more recent thermal tracer technique for estimating shallow flow velocities and investigating the effects of a wide range of hydraulic conditions on the correction factor used to determine mean flow velocity (Abrantes et al. 2018) (Fig. 13).

Measurement of Elements Related to Surface Runoff

Soil Temperature and Humidity

In each of the above-mentioned runoff-monitoring plots, two 1.5 m deep wells will be constructed to monitor soil moisture and temperature synchronously. Soil moisture and soil temperature sensors will be installed in adjacent wells at different depths. Soil moisture can be determined by a frequency domain reflectometer (FDR) using a calibrated soil moisture sensor equipped with a Theta-probe. Volumetric soil moisture can be derived from changes in the soil dielectric constant, converted to a millivolt signal, with an accuracy of ±2%. Soil temperature was monitored using a thermal resistance sensor sensitive to temperature changes in the range of -40 to 50°C, with an overall system precision of ±0.02°C. The thermal resistance sensors were developed by the State Key Laboratory of Frozen Soil Engineering in Lanzhou, China, using Fluke 180 series digital multimeters (Fluke Co., USA). The sensors had been even successfully used in other projects on the

Fig. 14 Photograph of (**A**) 30 cm diameter (inner) and 60 cm diameter (outer) double-ring infiltrometer, (**B**) 15 cm diameter (inner) and 30 cm diameter (outer) double-ring infiltrometer, and (**C**) Mariotte siphon developed to maintain a constant inner head in the infiltration rings (Gregory et al. 2005)

Qinghai–Tibet Plateau over the past 20 years (Wu and Liu 2004; Wu et al. 2002). All of the soil temperature and moisture data can be collected automatically once every 30 min by a CR1000 data logger.

Soil Infiltration Rate Measurement

Too many methods have been applied to measure infiltration rate like the ring infiltration method, hydrological method, artificial rainfall method, among which the classical double-ring infiltrometer stands out (Mathieu and Pieltain 1998).

Double-ring infiltrometer usually consists of two concentric metal rings (Fig. 14). The rings are driven into the ground and filled with water. The outer ring helps to prevent diver-gent flow. The drop-in water level or volume in the inner ring is used to calculate an infiltration rate. The infiltration rate is the amount of water per surface area and time unit which penetrates the soils. The diameter of the inner ring should be approximately 50–70% of the diameter of the outer ring, with a minimum inner ring size of four inches. The infiltration velocity was measured from the beginning of the experiment until a stationary regime, the steady-state infiltration rate (SIR) was reached. The steady-state rate was assumed to be reached when three consecutive similar measurements were observed after 90 min. Taking into account the spatial variability, three replicates were performed in each zone with a distance of 5–10 m between each other. In all cases, the land slope was less than 5% (Neris et al. 2012).

Evapotranspiration Measurement

This weighing lysimeter was constructed in 1990 and put into operation in 1991. It is placed in the middle of a 1.0 Ü 106 m^2 cultivated field. The basic components of the lysimeter are illustrated in Fig. 15. Component I is a steel oil cylinder with a surface area of 3.14 m^2 and a soil profiles with depth of 4.5 m overlying 0.5 m of fine sand. The aboveground part is 0.05 m in height. The steel cylinder wouldn't be cut into the soil until the lysimeter was constructed. Therefore, the lysimeter was filled by undisturbed soil. A neutron probe access tube (IV) is installed in the column. The soil column rests on a sensitive weighing system (V) capable of measuring the total mass of approximately 35 Mg to the nearest 60 g. A Mariotte system (II) is

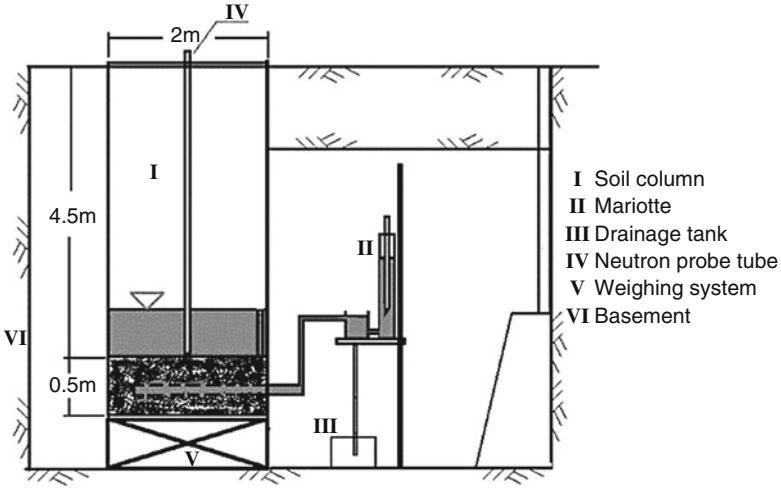

Fig. 15 The measured evapotranspiration in the lysimeter (Yucheng Comprehensive Experimental Station, Chinese Academy of Sciences, 1999) (Luo et al. 2003)

Fig. 16 A picture for the weighing lysimeter

connected to the soil column to control and record the water table inside, and measure the amount of water that is supplied to the soil column and/or leaks out of it. Gravity drainage is collected by a drainage tank (III). By recording the weight change of the soil column, water leakage from or water supply to the soil column, and the irrigation and/or rainfall amount, the total evapotranspiration, at certain time intervals, from the lysimeter can be obtained through a water balance approach. Generally, observations are made at 08:00 and 20:00 each day (Luo et al. 2003). The weighing system is calibrated every year. A picture for the in-situ weighing lysimeter is shown in Fig. 16.

General Modeling of Surface Runoff

Basic Concepts in Hydrological Models

Hydrological models have been developed to improve our understanding of surface runoff generated from complex watersheds, which should capture the essence of the physical controls of soil, vegetation, and topography on runoff production. Generally, there are three mechanisms generating surface runoff: (i) unsaturated surface runoff (Hortonian-type runoff), (ii) saturation-excess surface runoff, and (iii) return of subsurface storm flow, where the last is detectable in some cases already on the plot scale but becomes increasingly important when moving from the plot to the catchment scale and from the event to longer time scales. However, not all excess water generated by these mechanisms contributes to surface runoff because some is stored on the surface as depression storage (infiltrating after rain events) and detention storage (partly running off after events). Factors involved in the process of runoff, such as soil characteristics, vary extensively over small distances.

A modeling approach to simulate the physical processes of runoff would be ideal to investigate the effects of changes in a catchment on its generation, due to the spatial and temporal heterogeneity of the factors involved in runoff at catchment scale. The hydrological models generally integrate existing knowledge into a logical framework of relationships and rules. They can be used to be predictive tools for water resources management and to improve our understanding of environmental systems as a tool for hypothesis testing. Some models are more simplified than others but at the base of each model, there is a mathematical description that simplifies the factors that are being considered and that enables models to make quantitative predictions. The selection of a suitable model should depend on study objectives, additionally other factors such as data availability, money, and time should also be taken into account. Due to the differences in soil and climate characteristics of catchments, there is a growing awareness that catchments respond to rainfall in a variety of ways. Therefore, increasing the complexity of a model structure through emphasizing more on the physical basis of natural processes does not necessarily improve the model performance.

Classifications of the Model

The mathematical descriptions of hydrological models are simplifications of the actual processes of streamflow in nature. The models whether empirical, physical, or combinations of the two are therefore based on many assumptions. In general, surface runoff models can be classified from stochastic to deterministic models, from black-box or empirical to conceptual models, from lumped to physically based (white-box) distributed models, and from land surface to global hydrological models. In a stochastic modeling approach, randomness or uncertainty in the possible outcome of the model is permitted due to the uncertainty introduced by the input

data. Besides, both the input and output variables of stochastic runoff models are described in terms of a probability density distribution. On the other hand, deterministic models focus on the simulation of the physical processes involved in the transition from precipitation to runoff. They can further be divided into conceptual- and physical-based runoff modeling approaches.

The predictions obtained from lumped modeling approaches are single values, whereas the distributed modeling approaches make spatially distributed predictions. Lumped modeling approaches consider a catchment to be one unit and a single average value representing the entire catchment is used for the variables in the model. However, the use of such simple models tends to generalize details of environmental processes, which may result in the loss of both spatial and temporal information. The distributed models make predictions that are distributed in space allowing to assess the effects of land use/cover changes in a catchment on the rate at which runoff is generated. Nevertheless, making a certain model more physical based implies that the input parameters are also increased and are more complicated to attain. Most parameters are obtained through it may introduce some error into the model when the parameters are processed contributes to the overall inaccuracy of a model.

Conceptual Models

The empirical models were simple transfer functions describing a linear relationship between rainfall and surface runoff like models of the Green and Ampt (1911), Philip or Horton (Horton et al. 1940) type, and the CS curve number. Watershed-scale models dealing with surface runoff and soil erosion from arable land. Assuming that surface sealing during heavy rainfall events dominates runoff generation on partly bare soils, they often stick to Hortonian-type surface runoff generation approaches. The simplest case of such runoff models are index models, which assume a certain constant fraction of the total rain falling in a catchment becomes surface runoff, or there is a constant loss rate from the total rain falling in a catchment before surface runoff occurs. These models are simple ways of obtaining approximate runoff estimates and are still widely used. Larger-scale models typically use Green and Ampt or Philip approaches assuming that there is the existence of sharp wetting front having a constant matric potential and the wetting zone is uniformly wetted with a constant hydraulic conductivity the initial soil moisture conditions. The US soil conservation Curve Number Method, developed by the U.S. Department of Agriculture and Natural Resources through the analysis of runoff volumes from small catchments in the USA, is another simple empirical method for estimating the amount of rainwater available for runoff in a catchment. This type of model has little data demanding and is easy to apply. However, limited quantitative information can be obtained on how the model parameters are developed and their application to conditions for which they are not developed may lead to questionable results.

Process-Based Models

Distributed hydrological models take account of the spatial variability of climate, soil, vegetation, and terrain, which are able to make a series of hydrological processes interconnected, such as snow accumulation and melt, soil moisture dynamics, runoff generation, recharge to groundwater, and evapotranspiration. Despite their complexity, the distributed hydrological models are very helpful to study the changes in hydrological processes caused by human activities, such as deforestation, urbanization, and forestation. This feature also offers the potential to improve hydrologic predictions since these elements are divided into smaller units that are more homogenous than the whole watershed. In physical-based modeling approaches, the characteristics and properties of nature processes are based on the laws of conservation of mass, energy, and momentum. Thus, such types of models are complicated and demanding in their data requirement (Dingman 2002). Due to the fast development of 3S (RS/GPS/GIS) technology, the distributed hydrological models have been well developed during the last decades. A wide range of physical-based rainfall-runoff models are available today, such as HBV, TOPMODEL, and the SHE. The representative semi-distributed hydrological model TOPMODEL, developed in 1971, describes runoff generation process including both saturation excess and infiltration excess runoff according to topographic index derived from digital elevation model (DEM). After TOPMODEL, distributed hydrological models such as SHE (System Hydrologic European) and SWAT (Soil and Water Assessment Tool) are fully distributed and contain more complex hydrological processes. Although the distributed hydrological models have more solid physical base compared to the lumped models, these models often require a large number of parameters to run them and most of the parameters required are obtained through calibration, making such approaches expensive and time-consuming. So selecting models depends on objectives, application, and availability of data (Table 1).

General Vegetation Controls on Surface Runoff Processes

Vegetation controls surface runoff by means of its canopy, roots, and litter components to reduce raindrops energy effectively and thus redistribute rainfall (Gyssels et al. 2005). Vegetation changes will change the properties of the land surface, thus affecting the slope runoff process and soil moisture infiltration process. Therefore, it is of great significance to reveal the mechanism of hydrological response under the condition of vegetation change.

Vegetation can affect surface runoff by intercepting rainfall, changing kinetic energy of raindrops, increasing surface roughness and infiltration, improving soil physical properties, and directly fixing soil by root (Ju et al. 2007; Xi et al. 2008; Gan et al. 2010). Vegetation also has a considerable influence on the shallow soil flow, which is manifested in the soil reinforcement of the root system, the soil anchorage

Table 1 Summary of the models commonly used surface runoff simulation

Model type	Model	Country	Reference
Lumped model	AWBM	Australia	Boughton and Chiew (2003)
	GR4J	Australia	Perrin et al. (2003)
	HBV	Sweden	Bergstrom (1995)
	HEC	USA	Feldman (1981)
	HSPF	USA	Crawford and Linsley (1966)
	HYDROLOG	Australia	Porter and McMahon (1971)
	IHACRES	Australia	Jakeman and Hornberger (1993)
	Sacramento	USA	Burnash et al. (1973)
	SIMHYD	Australia	Chiew et al. (2002)
	SWM	USA	Crawford (1962)
	Tank	Japan	Sugawara et al. (Sugawara et al. 1986)
	Xinanjiang	China	Zhao (1992)
	SRM	Nordic	Martinec (1975)
Physical model	CEQUEAU	Canada	Morin et al. (2002)
	HYDROTEL	USA	Fortin et al. (Fortin et al. 2001)
	IHDM	USA	Calver et al. (1987)
	MIKE-SHE	Denmark	Refsgaard and Storm (Refshaard and Storm 1995)
	SHE	Denmark	Abbott et al. (1986)
	SLURP	UK	Kite (1995)
	SWAT	USA	Neitsch et al. (2002)
	SWMM	USA	Rossman (2009)
	TOPMODEL	UK	Beven and Kirkby (1979)
	WATELOOD	Canada	Kouwen et al. (Kouwen et al. 2002)

in the root system, the regulation of soil moisture, the soil support and dome, the load-bearing effect, root wedge effect, and wind transmission (Barker 1995; Morgan and Rickson 1995; Nordin 1995). Figure 17 depicts this process.

Effects of Vegetation Components on Surface Runoff

Canopy Layer Regulate Surface Runoff by Intercepting Rainfall

The canopy layer of forest vegetation distributes the precipitation for the first time. Larger interception capacity reduces the effective precipitation that the precipitation reaches the ground, reduces the raindrop's falling speed, and prolongs the duration of the precipitation and runoff. When the vegetation canopy interception reaches the limit value, it will no longer affect the net rainfall and redistribute to the precipitation. This effect has continued.

The results of most of the related studies show that the canopy layer interception rates of different forest types are as follows: coniferous forest<broad-leaved forests, deciduous forest<evergreen forest, single-layer forest<stratified heterogeneous

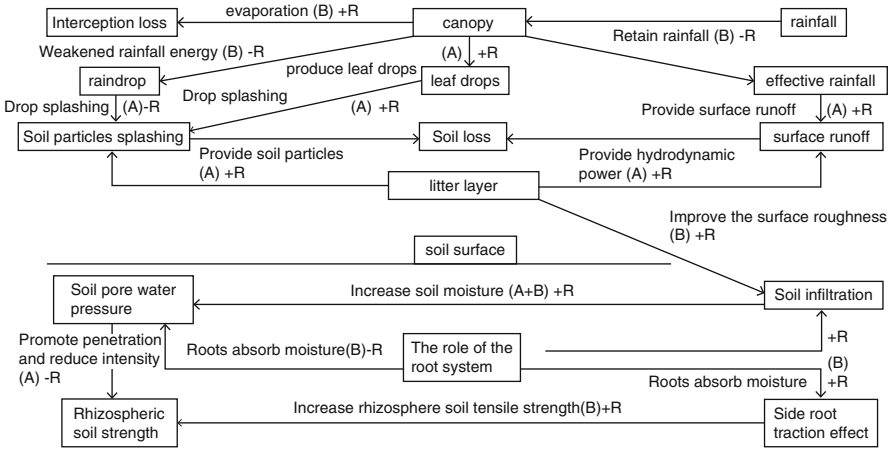

Fig. 17 A conceptual model of the comprehensive effects of the forest on slope protection. A: Adverse effect, B: Benificial effect, +R: accelerating action, -R: weakening action (Zhou 2000)

forest, and pure forest<mixed forest. Canopy density has a greater impact on canopy interception, and dense canopy offers higher interception rate (Tang 2012). The canopy layers of different forest stands have different effects on the kinetic energy of raindrops. Taking *Huashan pine* forests as an example, when the canopy height exceeds 7 m, the impact of the canopy layer on the kinetic energy of the raindrops becomes negligible (Lei 1997; Yu et al. 2006, Yu et al. 2010). Hierarchical vegetation communities protect soil better than monolayers and reduce water erosion.

Hydrological effects of forest canopy under different rainfall intensity are also different. When the rainfall intensity is small, the effect of branches and leaves of canopy on the accumulation of rainfall and raindrops is very prominent. The kinetic energy of raindrops under forest rain and the splashing effect on soil are also obvious (Xie et al. 1994; Wang and Zhang 1998; Zhou 2000). However, when rainfall intensity is larger, the canopy interception is more obvious.

Plant Roots Improve Soil Corrosion Resistance, Soil Permeability, and Soil Stabilization

Vegetation can effectively prevent soil erosion during runoff (Liu et al. 2010). The role of plant roots in soil erosion control is much larger than that of aerial parts, and its role cannot be ignored. The root system's entanglement and distribution in soil are the key factors affecting the degree of soil hydraulic properties, including the density, distribution, and branching characteristics of the root system (Shi et al. 2009).

Soil mechanics composition, structure, porosity, water content, and other indicators all affect the permeability of soil. Plant root system has a great influence on soil physical properties and therefore directly affects the soil infiltration capacity. Some researchers believe that the effect of plant roots on soil infiltration capacity is mainly reflected in the effect of the root system on the bonding of single soil, the dispersion

of solidified compacted soil, and the decomposition of the root system itself to humus on the soil aggregate structure and pore condition (Zhu and Ren 1992).

Root growth can improve the friction between roots and soil, root system. At the same time, the root system itself has the ability of antishear and anti-pull. Combining these two points, the root system can play a role of stabilizing the soil. Plant roots are integrated with the soil during the growth process, developed and integrated into a soil-plant-atmosphere continuum, which plays a role in soil consolidation (Yang et al. 1996).

The Litter Layer Again Intercept Rainfall, Thus Prolonging Runoff Formation Time

The effect of litter layers on slope runoff is mainly manifested in two aspects. First, its water storage and holding capacity can prolong runoff and improve soil infiltration capacity; in addition, the presence of litter increases the effective surface roughness, which reduces runoff flow rate to prevent soil erosion (Zhang et al. 2005; Hu et al. 2008).

Effects of Vegetation Covers on Surface Runoff

Changes in vegetation coverage will change the underlying surface properties, which has a significant impact on the slope runoff process. Loss of vegetative cover may lead to the formation of soil seals that increase runoff during the early stages of seal development (Singer and Le Bissonnais 1998).

Quantitative studies under different environmental conditions have demonstrated the positive effect of vegetative cover in reducing water erosion at small scales, with increased soil infiltration accompanied by surface runoff diminished (linearly or exponentially) (Cerda 1999; Dunne et al. 1991; Francis and Thornes 1990; Muñoz-Robles et al. 2011; Quinton et al. 1997; Reid et al. 1999). Vacca et al. (2000) studied runoff in three areas under different land uses (abandoned grazing land, burned machia, and Eucalyptus sp.) and found that different amounts of runoff result from different land uses. The highest runoff was found under Eucalyptus sp. (135 mm), followed by abandoned grazing land (45.25 mm) and burned machia (30.45 mm). Reid et al. (1999) noted that the total runoff was significantly different among three types of land patches, the highest being from bare intercanopy patches, the intermediate being vegetated intercanopy patches, and the lowest being canopy patches. In another study, the decrease in canopy cover density as a result of overgrazing led to rapid runoff yield in rangelands (Oztas et al. 2003).

Seeger (2007) confirmed that increased vegetation coverage can effectively reduce runoff and sediment yield. Eshghizadeh et al. (2015) selected erosion sites in northeastern Iran as the target region and kept monitoring the soil erosion during the period of 2008 to 2015. After analyzing major natural factors affecting runoff and soil erosion in semiarid areas, he concluded that the vegetation coverage has a linear relationship with runoff (Fig. 18).

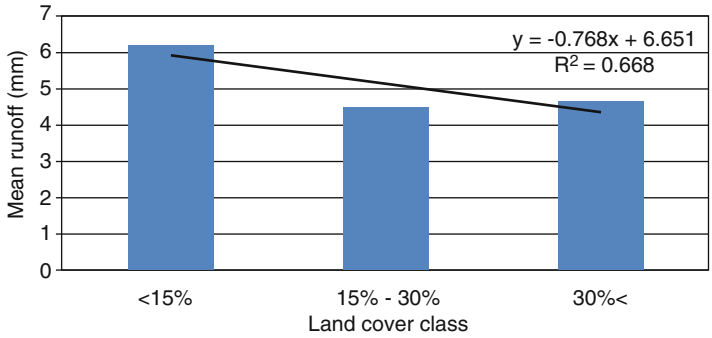

Fig. 18 Mean runoff in each class of land covers (canopy and litter) (Eshghizadeh et al. 2015)

Loss of vegetative cover as a result of human activities such as overgrazing and deforestation leads to the formation of soil seals (Singer and Le Bissonnais 1998) that increase the risk of runoff (Al-Jubeh 2006; Singer and Le Bissonnais 1998; Snyman and Du Preez 2005). Snyman and Preez (Snyman and Du Preez 2005) and Al-Jubeh (2006) observed that rangeland degradation usually leads to increased surface water runoff due to decreased plant cover, reduced aggregate stability, reduced soil fertility, and decreases in the soil water content in all soil layers. In another study, Merzer (2007) reported that bare plots produced significantly more runoff as compared to variety of vegetative plots.

Actually, vegetation can function to reduce runoff yield only if coverage has achieved to a certain threshold. The optimal vegetation coverage refers to the one which can make the soil loss less than the allowable soil erosion. Vegetation coverage has two different definitions of critical coverage and effective coverage. When the critical coverage is exceeded, the effect of vegetation coverage on surface runoff would not increase with the increase of coverage, in addition to the heavy rainfall (Li et al. 2005). When the rainfall intensity exceeds the critical threshold of rainfall, the effect of vegetation reduction would decrease, and the impact of coating on the runoff yield would be very small (Yao et al. 2011). Zhu et al. (2010) studied the effects of herbaceous vegetation cover on slope runoff erosion by using artificial simulated rainfall in the field. The results show that when vegetation coverage is 0% to ~60%, the increase of vegetation coverage can effectively reduce runoff yield and sediment yield. When the vegetation coverage is more than 80%, the influence of the increase of coverage on the runoff coefficient is weakened, and the influence of vegetation on runoff and sediment yield tends to be stable. Therefore, the critical vegetation coverage is 60–80%. Through the artificial simulated rainfall experiments, Zhao et al. (2015) found that the vegetation coverage would have a significant impact on soil moisture content and runoff. When the vegetation coverage reaches 18%, the time to stabilize seepage is shortened, and the runoff coefficient significantly decreases (Table 2). However, in the case of heavy rainfall, the runoff yield is still fast even though the coverage of the slope land reaches more than 50% in Loess Plateau.

Table 2 Runoff coefficient under different vegetation fractional coverage (Zhao et al. 2015)

Site number	Vegetation fractional coverage (%)	Runoff coefficient		Decreased runoff compared to bare soils (%)	
		5 min	10 min	5 min	10 min
$2^{\#}$	0	0.55	0.57	0	0
$3^{\#}$	11	0.37	0.48	32.73	15.79
$4^{\#}$	18	0.23	0.28	58.18	50.88
$5^{\#}$	43	0.29	0.37	47.27	35.09
$6^{\#}$	53	0.20	0.26	63.64	54.39

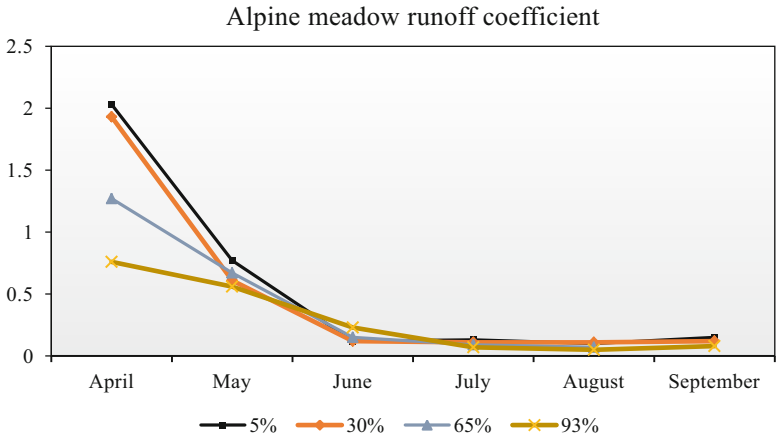

Fig. 19 Seasonal dynamics of surface runoff in alpine meadow under different vegetation coverage (Wang and Zhang 2016)

Fan (2014) studied the variation of runoff under different forest densities and grassland coverage. Both the forestland and the grassland significantly delayed the runoff time and effectively controlled the slope infiltration process. With the increase of vegetation coverage, stream intensity decreases. As the process of surface freezing and thawing profoundly affects the surface runoff process, the process of runoff generation in the cold area is inevitably different from that in the nonfrozen area. Wang and Zhang (2016) revealed the runoff generation mechanism of alpine meadow and alpine swamp in permafrost watershed of central Tibet Plateau from the observations in two catchments. Under different coverage conditions, seasonal dynamics in the runoff coefficients of alpine meadows and high-cold swamps can be seen in Figs. 19 and 20. Surface runoff process in the cold area is significantly different from the seasonal dynamic in the nonfrozen area because of the influence of surface freezing and thawing process.

In summary, depending on different vegetation coverage, runoff yield patterns varied. When vegetation has achieved to a certain threshold, the larger the vegetation coverage, the lesser the rainfall runoff will be. A common method for decreasing runoff is via stable and suitable vegetative cover (Chaplot and

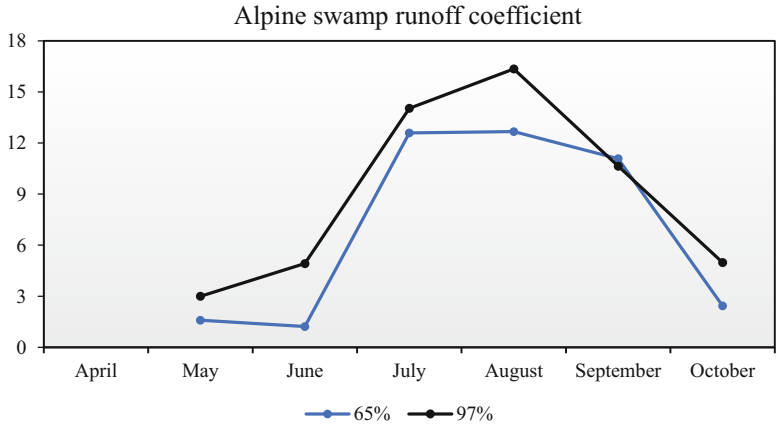

Fig. 20 Seasonal dynamics of surface runoff in alpine swamp under different vegetation coverage (Wang and Zhang 2016)

Le Bissonnais 2003; Dunjó et al. 2004; Kothyari et al. 2004; Mohammed 2005; Zhang et al. 2004).

Effects of Vegetation on Soil Water Infiltration

Infiltration is the process whereby water enters the soil and adds to the total soil moisture (Philip 1957a; Warrick 2003). Soil infiltration is an indispensable physical parameter to describe the soil characteristics and a critical process to link other hydrological components (precipitation, surface water, soil water, groundwater) during phase changes of water cycles. There are a number of factors that affect infiltration, including the vegetation, slope, rainfall regime, soil texture, soil structure, and so on (Leonard and Andrieux 1998). It is of great significance to conduct studies of relations between soil water infiltration process and vegetation changes to reveal hydrological response mechanism under the circumstances of changing vegetation.

Several models, including Green-Ampt equation (Green and Ampt 1911), Kostiakov equation (Kostiakov 1932), Hortan equation (Horton 1941), Philip equation (Philip 1957b), Holtan equation (Holtan 1961), and Smith equation (Smith 1971), can be used to simulate the processes of soil infiltration. The importance of vegetation cover in maintaining and improving soil stability and permeability is well known and has been discussed extensively (Branson et al. 1972; Colman 1953). The mechanism of how vegetation affects soil infiltration can be expressed as follows. One option is the cover may intercept raindrop energy and prevent surface sealing. Alternatively, vegetation increases surface roughness, which changes the flow-routing pattern and erosion processes (Li et al. 1992; Yu et al. 2006). Lastly, vegetation changes hydraulic properties of the underneath and surrounding soil by modifying the structure of the soil pore spaces as a result of the formation of the root

system (Thompson et al. 2010a, b). Most studies revealed that soil hydraulic conductivity under vegetation would be 3–5 times higher than the bare soil (Bhark and Small 2003; Bromley et al. 1997; Dunkerley 2000; Titus et al. 2002).

Researches about the processes that generate vegetation-infiltration capacity feedbacks have been widely explored in drylands dating back to 1930s. However, at the initial stage, the theory of how vegetation affects infiltration is not well developed. For example, Johnson and Niederhof (Johnson and Niederhof 1941) failed to discover any simple relationship between vegetation cover density and infiltration capacity measured with infiltrometers, whereas Smith and Leopold (1942) documented large changes in infiltration with only modest changes in vegetation density in Pecos River watershed in New Mexico. Since then, detailed studies of the effect of plants on infiltration were conducted by many others (Duley and Domingo 1949; Dyksterhuis and Schmutz 1947; Woodward 1943). Experiment by Marston (1952) in the Davis County Experimental Watershed demonstrated that vegetation cover of 65% or more significantly increased infiltration. Lyford and Qashu (1969) measured constant rates of infiltration with a double-ring cylinder infiltrometer (with 11 and 30 cm diameter rings) at different distances from three desert shrub in a 45 cm deep sandy loam. Each plant stem was surrounded by a topographic mound (of unreported height) with a diameter approximately equal to that of the crown cover. The mounds were covered with annual weeds. The results show a strong lateral gradient in infiltration capacity (Fig. 21). Johnson and Gordon (1988) also demonstrated an approximated doubling of 30-min average infiltration rates beneath shurubs, as compared with grassy areas between the shrubs.

A complete review of the relationship of vegetation to infiltration in semiarid regions is summarized by Branson et al. (1981). On hillslopes of natural length and roughness, vegetation plays an important role in decreasing the average velocity of flow, increasing its residence time, and allowing significant post-storm infiltration to decrease runoff volumes (Dunne and Dietrich 1980) and created a simple water balance model to predict soil infiltration based on 4 years field observations.

In recent years, numerous studies have also been carried out, focusing on the mechanism of soil infiltration influenced by vegetation changes. McLeod et al. (2006) researched the soil water regimes of a Brown Chromosol on the Northern Tablelands of NSW, Australia, under three pasture types and noted that the vigorous phalaris plus white clover pasture yielded the greatest potential for water storage. Yi and Mińgan (2007) showed that when other conditions are the same, the higher the vegetation coverage and the larger the initial and steady infiltration rates, the greater the recharge coefficient of precipitation infiltration. The infiltration rates and cumulative infiltration amount with different coverage can be expressed as power function relations with time. Wang et al. (2008) studied the influence of vegetation on infiltration and redistribution patterns with the aim of identifying tools for rebuilding desert ecosystems and suggested that vegetation had a significant effect on infiltration and redistribution patterns in stabilized sand dunes. Schwartz et al. (2010) studied soil water redistribution under sweep tillage and in untilled control plots and found that tillage with a sweep of 0.07–0.1 m significantly reduced net water storage at soil depths above 0.3 m but did not affect the water content at depths $\geq$0.2 m.

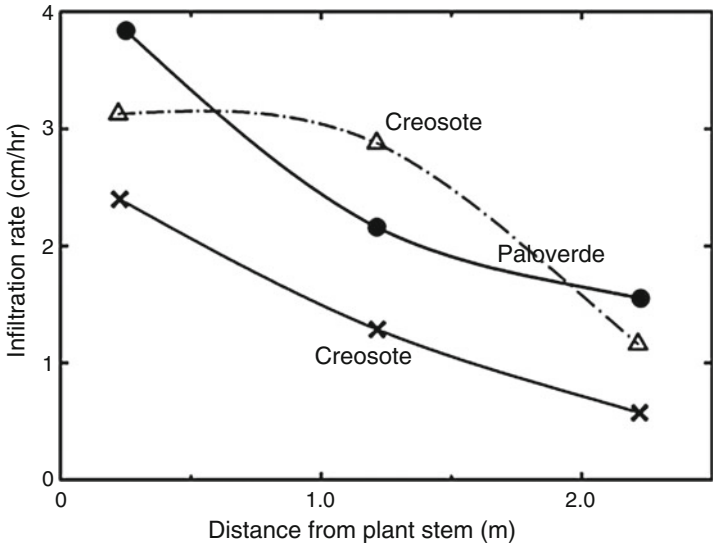

Fig. 21 Variation of infiltration capacity with distance from the stems of desert shrubs after (Lyford and Qashu 1969)

Numerous mathematical simulations of the infiltration process have also been conducted. Zhou et al. (2015) compared the simulation results of Horton, Philip, Kostiakov, and Green-Ampt model with in-situ measurements. Results revealed Hortan equations described the infiltration characteristics much better than the others. By artificial rainfall, Zhao and Wu (2004) concluded that Smith-Parlange equation can better capture the slope infiltration processes than Hortan and Kostiakov equations.

In summary, with the increase of vegetation coverage, there exists an obvious increase of soil infiltration whereas when the soil moisture content, rainfall amount, and rainfall density have achieved to a large extent, the impact degree of vegetation coverage decreased.

Observation of Vegetation Impacts on Surface Runoff: Precipitation Interception

Concept of Precipitation Interception

Precipitation interception by vegetation is an important fraction of water cycles, which is collected and temporarily stored on vegetation before being evaporated. Many studies have shown that interception losses are of major importance in influencing the water yield of forested areas relative to deforested area and other vegetative cover area such as shrubs, crops, and grass (Crockford and Richardson 2000). Better understanding of the interception process will allow reliable estimate

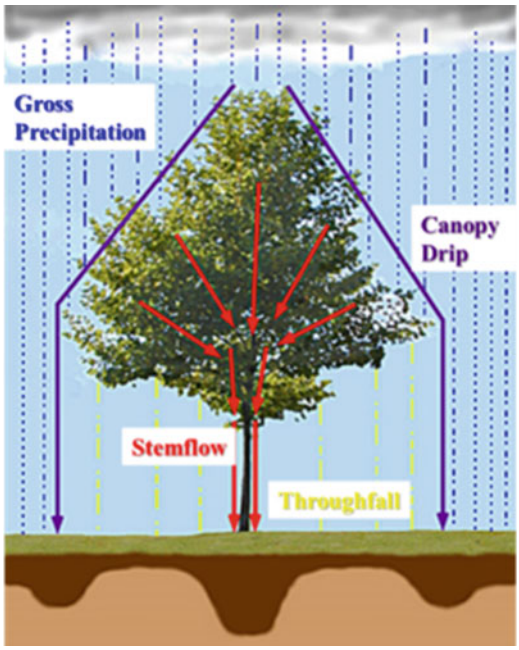

Fig. 22 Modification of falling precipitation by vegetation. The relative quantity of precipitation entering the soil is indicated in dark brown (Pidwirny 2006)

of its impact on surface runoff. Vegetation type, ground cover, and climate condition affect the amount of precipitation that reaches the ground surface.

Precipitation, i.e., gross precipitation (P) that input from above the canopy, can be partitioned into three fractions (Fig. 22): (i) that remains on the vegetation and is evaporated after or during rainfall (interception, I); (ii) that which flows to the ground via trunks or stems (stemflow, SF); and (iii) that which may or may not contact the canopy and which falls to the ground between the various components of the vegetation (throughfall, TF). The mass balance of partitioning of rainfall is generally expressed as:

$$I = P - TF - SF \tag{18}$$

Throughfall and stemflow are the two hydrological processes responsible for the transfer of precipitation and solutes from a vegetative canopy to the soil (Levia and Frost 2003), which typically account for 70–90% of the incident gross precipitation in temperate forests.

Precipitation Interception Effect on Surface Runoff Redistributing

Canopy interception of precipitation plays an important role in modulating the hydrologic process and water budget. Canopy interception indirectly influences the distribution ratio of runoff and infiltration by changing the amount of rainfall that

reaches the ground, delaying the time to runoff and decreasing the flow volume and flow rate (Love et al. 2010; Zhang et al. 2016). It is usually described as interception rate (IR), which is the ratio of canopy interception divided by total rainfall at certain time intervals (Gavazzi et al. 2016). Interception rates are influenced by meteorological conditions such as wind speed and direction, evaporation rate, rainfall rate and duration, and canopy structure.

Influence of Vegetation Species

In the early twentieth century, Horton (Horton 1919) presented one of the first detailed analyses of rainfall interception across species and found that conifers intercepted more rainfall than hardwoods, but only hardwoods exhibited seasonal differences. Rates have exhibited high variability between and across species, the spruce-fir-hemlock forest type has been shown to have the highest canopy IR followed by pines and then hardwoods (Helvey and Patric 1965). Higher streamflow rates in beech (*Fagus sp.*) versus spruce (*Picea sp.*) dominated watersheds. Global estimates and spatial differences in the distribution of interception over different ecosystems showed interception loss was responsible for the evaporation of 13% of the total incoming rainfall over broadleaf evergreen forests, 19% in broadleaf deciduous forests, and 22% in needleleaf forests (Miralles et al. 2010). It was also found that interception was higher in dryer regions, indicating greater impacts on water resources (Soto-Schönherr and Iroumé 2016). However, unless under a large density, the effect of rainfall interception in grass is not as obvious as in other types of plants because mostly grass is low and short, whose leaves are small and soft and cannot hold much water (Zhang et al. 2016). Interception rate of shrub-grass layer in Liupan mountain region was about 1.8–12.6% (Liu et al. 1994). The clearing of native forest and establishment of grass on a small catchment in southwest of Western Australia resulted in a large streamflow increase (30% rainfall yr^{-1}), which was brought about by a decrease in transpiration and interception loss (Ruprecht and Schofield 1989). Greater amounts of vegetation and accumulated litter generate greater resistance to runoff, which decreases with decreasing grassland coverage (Zhang et al. 2016).

Influence of Meteorological Conditions

In study on evergreen broad leaves forest in east of coastal China, Peng et al. (2014) suggested that lag time of stemflow was about two times longer than throughfall and canopy interception contributed the rainfall redistribution up to 25–31%. The percentage of rainfall intercepted decreased as rainfall rate increased. The storage capacity of foliage was between 0.5 to 1.8 mm per storm. Interception rates averaged 25% during heavy rains of long duration but could be as high as 100% during light rainfall events when total rainfall did not exceed the storage capacity (Horton 1919). Peng's results (see in Fig. 23) support the well-established exponential decay relationship between the gross precipitation and the interception percentage after the canopy is saturated (Peng et al. 2014). Even the intercepted snow during the snow accumulation season could be removed from the canopy via three pathways: sublimation, mechanical removal (sliding leading to mass release), and meltwater

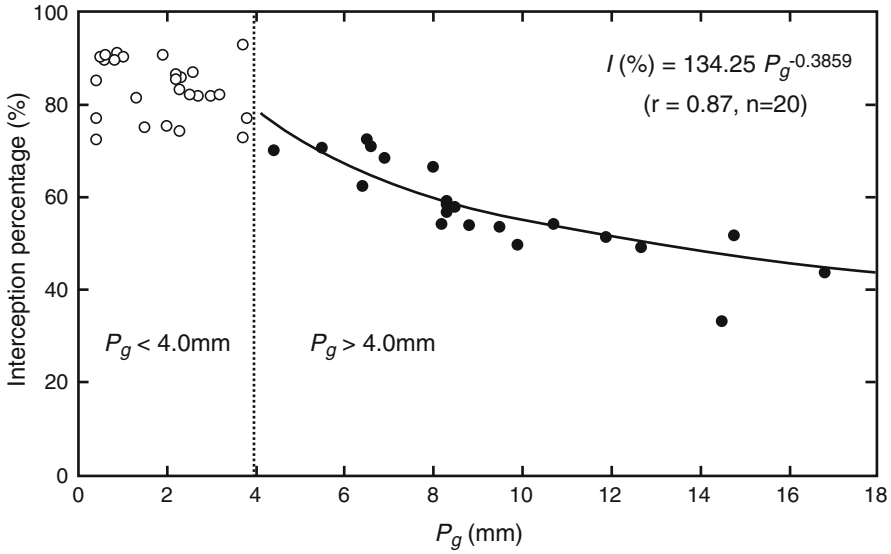

Fig. 23 The relationship between gross precipitation (P_g) and interception percentage (I) (Peng et al. 2014)

drip, which results in reduced snow water equivalent quantities and delayed lag time to surface runoff (Suzuki et al. 2008). During the snow accumulation season, a portion of the snowfall is intercepted by the forest canopy and sublimates or melts. Snowfall interception is important for understanding the water and energy balance of snowy watersheds (Suzuki et al. 2008).

Moreover, the decade-long data of canopy rainfall interception, study found that interannual variability of canopy interception is higher than reported in short-term studies (Gavazzi et al. 2016). It indicates uncertainties of rainfall interception should also be considered on surface runoff research and accurately predicting the hydrologic impacts of management and climate change.

Measurement for Interception

Interception cannot be measured directly but can be calculated through observation of gross precipitation, throughfall, and stemflow as in Eq. (18).

Gross Precipitation Measurement

As interception is the difference between gross and net rainfall, generally expressed as percentage of gross rainfall, accuracy in measurement of both parameters is critical (Crockford and Richardson 2000). Problems in measurement of gross rainfall are commonly ignored comparing with the measurement of net rainfall (throughfall and stemflow). The horizontal angle between the rain gauge and the top of the

nearest trees was smaller than 45°, so little disturbance on gross rainfall measurement was caused by its surrounding environment (Asdak et al. 1998). However, sites for forest studies seldom have well-positioned rainfall gauges (Dohnal et al. 2014; Peng et al. 2014; Zimmermann et al. 2010). Aerodynamic effects both on canopy level gauges and on gauges in forest clearings are likely to lead to systematic errors in the measurement of rainfall, i.e., gauges can either underestimate or overestimate owing to wind-induced loss (Crockford and Richardson 2000; Robinson et al. 2004) or receive water blown from the canopy if placed close enough to the canopy, respectively. Wind-induced underestimation of precipitation is more likely with small drop-size rainfall. Larger drops have more momentum and are less likely to be blown away from the collector. Accurate measurement of precipitation is difficult when the study area is within a larger forest and gauges have to be placed above the canopy or in gaps in the canopy; the latter can result in overestimation of precipitation as a result of blow-in from the nearby higher tree crowns and the former can experience wind loss (Crockford and Richardson 2000). Therefore, the information of precise position of rain gauge in relation to the experimental plot, and where the gauge is noted as being in a clearing, the size of the clearing and the location of the gauge are important, because small errors in precipitation measurement can lead to large errors in the estimation of interception.

Throughfall Measurement

The accurate estimation of throughfall is generally difficult among the whole measurement of interception. The great error will be happened due to the spatial canopy heterogeneity of high forest, shrubbery, and even some grass ecosystem that may cause spatial variability of throughfall. Therefore, the search for robust sampling schemes, from size of devices (Crockford and Richardson 2000) to sampling design (Zimmermann et al. 2010) has attracted some interest in recent decades.

Collector Devices

Usually, the variability problem can be overcome by increasing sampling area of interception observation by using large plastic-sheet (Calder and Rosier 1976) or mostly trough-type net rainfall collectors (see in Fig. 24) (Fan et al. 2014; Herbst et al. 2006; Peng et al. 2014; Silva and Okumura 1996). Moreover, sampling strategy is also developed for accuracy purpose. (Zimmermann et al. 2010) studied throughfall by different sampling designs and variable sample supports (see in Fig. 25). Large number of collectors will be required to estimate mean throughfall, particularly for small events for a relative error limit of 20%. A larger enough sampling area is also needed for estimating throughfall of an uneven density canopy, i.e., more collectors are required. In order to control the error limit of 5%, several to dozens, even up to163 of rain gauges (Llorens and Domingo 2007), were designed to throughfall collection according to variable canopy characteristic (Czarnowski and Olszewski 1970), seasonal variation (Helvey and Patric 1965), and the area of sampling sites. There is even equation to determine the number of collectors required to estimate throughfall volume according to characteristic of canopy heterogeneity (Carlyle-Moses et al. 2004; Puckett 1991).

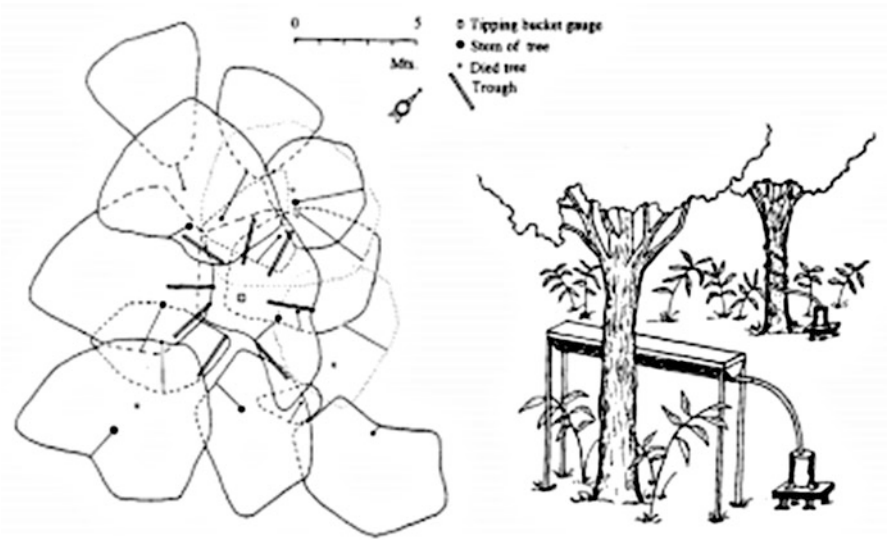

Fig. 24 Vertical crown projection map and layout of instruments of trough-type collector and stemflow collector in a natural oak forest (Silva and Okumura 1996)

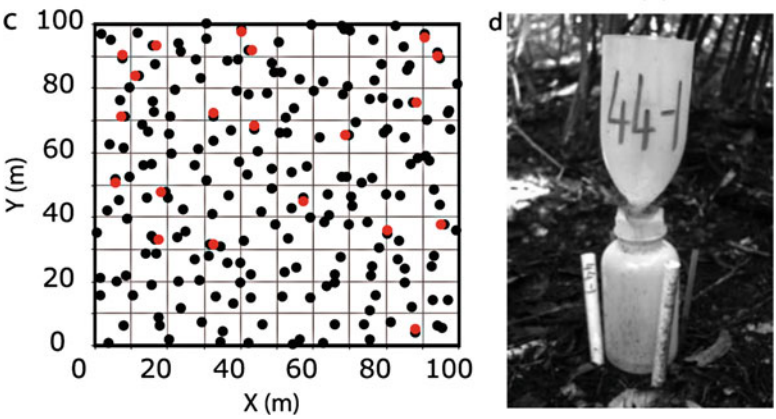

Fig. 25 (**a**) The close-up view of the 1 ha sampling area shows the location of sampling points (dots). Different colors of dots indicate collector placement according to different sampling strategies, that is, black dots refer to locations that were chosen according to a design-based sampling strategy, whereas red dots mark locations selected by a model-based strategy. (**b**) The photo shows one of the funnel-type samplers (Zimmermann et al. 2010)

Sampling Location Design

In addition to the difference of collectors, sampling location and design will also influence the result. Random sampling is the method that gauges are randomly located within a fixed plot or relocated periodically (Link et al. 2004). It will provide

even coverage of the entire plot while capturing the full range of variation. Systematic sampling is the method that gauges are evenly distributed in regular grids or equidistance (Herbst et al. 2006; Xu et al. 2010). There is no significant difference between two methods according to comparative studies (Holwerda et al. 2006; Zimmermann et al. 2010). The random relocation of small, funnel-type collectors during the sampling period, subject to some assumptions, improves the efficiency of sampling estimates by increasing the spatial coverage. However, for the common problems of estimating throughfall for particular events, there is no consensus on the best strategy, but there is recognition that estimates of this variable are subject to considerable sampling error, and that these errors will propagate when the estimates are used in subsequent modeling (Zimmermann et al. 2010). Study showed that interception rate had a range between 3% and 25% among 23 subplots of lowland tropical forest canopy even in the same rainfall intensity (Manfroi et al. 2006). Therefore, location design will only reflect the rainfall interception of sampling plot scale. The estimation of spatial interception amount will be limited if the size and location of the observed plot cannot represent spatial feature of whole canopy.

Stemflow

Accurate measurement of stemflow is even more difficult, but in some areas, stemflow is a very small proportion of net precipitation and sometimes is not measured. In some forests, however, stemflow can be large enough to warrant special care (Crockford and Richardson 2000; Zhang et al. 2007). There is no standard protocol to adequately sample stemflow volume, likely the result of the diverse vegetation cover from which stemflow is collected and the differing objectives among stemflow studies (Levia and Frost 2003). Stemflow, however, is usually captured by circumferential collars which are formed by a small tire wrapped around the tree, attached with galvanized iron nails filled by polyurethane foam and finally sealed with neutral silicone sealant (Crockford and Richardson 2000; Dohnal et al. 2014; Dunkerley 2000). Then the stemflow is diverted to collection bin or tipping-bucket gauge to measure (see in Figs. 24 and 26). Following Hanchi and Rapp (Hanchi and Rapp 1997), the tree-level stemflow was upscaled to the stand-level stemflow for both forest stands using Eq. (19).

$$S_f = \sum_{i=l}^{n} \frac{S_n \cdot m}{A \cdot 10^4} \tag{19}$$

where S_f is the upscaled stemflow depth (mm) for a specified stand area of A (m^2), n is the number of diameter at breast height classes, and S_n is the average stemflow volume (ml) collected from m trees in the diameter at breast height classes.

Experiment on Grassland and Meadow

The above methods are usually used on study of trees and shrubs. Theoretically, those methods can be used in study on rainfall interception of grassland. However, it is difficult to design the experiment to measure the throughfall and stemflow of

Fig. 26 Stemflow collector consisting of plastic tubing and a collection bottle. Left figure for shrubs (Li et al. 2008) and right figure for trees (Germer et al. 2010)

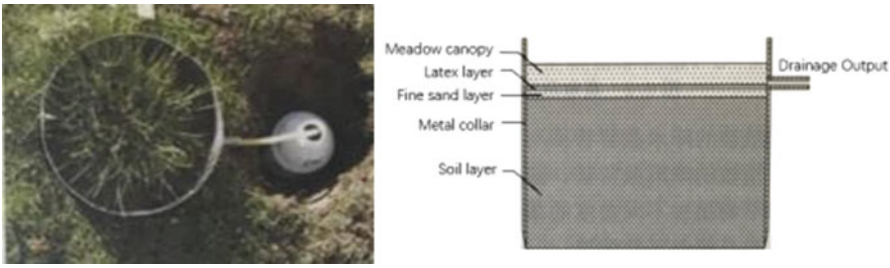

Fig. 27 Rainfall interception observation device for meadow (Wang and Zhang 2016)

dwarf and creeping growth grass. There are not recognized common experiment methods for the interception of grass and meadow study. One way is measuring throughfall and stemflow as one part together, using water balance to calculate the interception amount by the difference of gross precipitation and drainage output. According to Corbett's study (Corbett 1968), an improved device (see in Fig. 27) was designed and used for hydrological study in typical Swamp meadow and Alpine meadow in Tibetan Plateau (Li et al. 2012). A certain size metal collar was driven into soil to seal the soil surface. A layer of fine sand was sifted onto the soil to provide a uniform, sloping surface for drainage. Then soil surface was sealed with the neoprene latex emulsion. A drain carried off the throughfall and stemflow when precipitation happens.

Other researchers observed the interception directly by measuring the rainfall storage capacity. This method is based on measurement of water retained by vegetal entities and the up-scaling of these measurements using the determination

of the surface of canopy feature (Li et al. 2009; Liu et al. 2015). The leaves and stem were randomly selected and taken back to laboratory, weighted to obtain fresh weight. Then they were maintained in the water for certain times (Llorens and Gallart 2000), reweighed to obtain wet weight when no more droplets. Water storage capacity, i.e., interception, was calculated by the difference of weight before and after soaking.

Interception Model

The various components of the rainfall interception process have been measured and modeled for many vegetation types. Apart from allowing extrapolation of measurement results in space and time, interception models also provide insights into the mechanisms of the interception process (Muzylo et al. 2009). Empirically derived relationships between interception loss and gross rainfall highly depended on species character of the interception process, which cannot be confidently applied where conditions are distinctly different. Conceptual model, i.e., physically based model which describes interception as a process, has been paid more attention due to its robustness in physics and less need for calibration of empirical coefficients (Cui and Jia 2014). To predict interception losses using readily available meteorological variables, researchers have developed over 15 physically based interception models.

Almost all the physically based models have been derived from two basic interception models: Rutter-type model that deals with the interception of rainfall drops using probability distribution and Gash-type model that deals with the redistribution of rainfall volume using a mass balance equation. The Rutter model represents the interception process by a running water balance of rainfall input, storage, and output in the form of drainage and evaporation (Rutter et al. 1971). The Gash model represents rainfall input as a series of discrete storms that are separated by intervals sufficiently long for the canopy and stems to dry completely, during which three phases can be distinguished – canopy wetting-up, saturation, and drying (Gash 1979). Subsequent two kinds of models have been improved. Muzylo et al. (2009) compared these models and found the original and revised Gash's analytical models to be the most commonly employed.

The input rainfall values of temporal resolution is from 10 min (Massman 1983) to daily (Mulder 1985) or mostly hourly (Cui and Jia 2014; Gash 1979; Rutter et al. 1971). The total number of model parameters varies considerably from model to model. In the case of the single-layer models, the number varies from 2 to 7, and in the case of the multilayer models, from 8 to 16 for stands comprising two layers (cf. Table 1 in Muzylo et al. (2009)). The models include parameter representing the storage of intercepted rain in the canopy or, to be more specific, the threshold amount of rain that can be stored in the canopy. Whereas, the analogous designations of this storage threshold are misleading, because its exact definition may differ significantly between models. Models also include a parameter describing the structure of the canopy. The bulk of the Rutter- and Gash-type models employ the free throughfall coefficient to partition the throughfall.

Satellite remote sensing observations can provide land surface information with high spatial and temporal resolution. Unfortunately, estimate of interception loss at regional scale using remote sensing information is not straight forward. Empirically based models have been applied to remote sensing observations for regional estimate of interception evaporation (Cui and Jia 2014). Nowadays, remote sensing can provide many variables or inputs needed by the physically based sophisticated models, for instance LAI, fractional vegetation cover (FVC). More and more attempts have been made in applying these satellite observed parameters to interception models, since there are still a few critical parameters which cannot be directly derived from remote sensing observations, e.g., canopy storage capacity, trunk storage capacity, and the proportion of the rainfall diverted to stemflow.

Observation of Vegetation Impacts on Surface Runoff: Root System

Surface runoff initiation is the result of rainfall intensity exceeding soil infiltrability, thereby leading to temporary saturated conditions at/near the soil surface (Cantón et al. 2011). Therefore, soil infiltrability should be regarded as the first scale of analysis. Soil structure in the top soil layers is particularly critical as it dominates water transport in the saturated and near-saturated range (Creswell et al. 1992; Bronick and Lal 2005). Plant roots are key drivers of soil structure enhancing aggregate formation and stability and improving soil shear strength (Haynes and Beare 1997; Kavdır and Smucker 2005; Gyssels et al. 2005; Baets et al. 2008). Root-induced macropores are of particular importance for runoff mitigation due to their large diameters and high connectivity, enhancing rapid rainfall infiltration and percolation to deeper soil layers (Cresswell and Kirkegaard 1995; Ghestem et al. 2011; Horn and Smucker 2005; Suwardji and Eberbach 1998).

Plant effects on soil structure are species dependent. For annual plants root diameter was shown to be an important trait for root induced pore formation, particularly in soil with high mechanical resistance (Bengough 2012). Legume species with coarse root axes created substantially more macropores compared to fine rooted species (Bodner et al. 2013).

Measurements of Root Parameters

The parameters commonly used to express root growth and distributions are number, weight, surface, volume, diameter, length, and the number of root tips (Bohm, 1979). The manner in which the root data is best expressed should be considered before starting an experiment. Not only the research aim but also the time and labor needed for the determination of the root parameter which has been chosen must be considered.

(1) Root number
Counting root number is the common procedure when working with the core-break method, profile wall methods, and glass wall methods. Root numbers counted in the different soil layers generally give a good impression of the rooting density in a soil profile. In studied where the entire undamaged root system of a single plant can be extracted, the number of main and lateral roots is counted to provide an estimate of their total length. Although root number is not an ideal parameter, as long and short roots are regarded and counted as equal units, high correlations with other root parameters are possible (Melhuish 1968).

(2) Root weight
Root weigh is the most commonly used parameter for studies of root growth in response to environment. Generally, the washed roots are dried and then their weight is determined. If root weight is to be determined in an ecological study, dry weight should be preferred. To determine dry weight, the washed and cleaned roots are dried in an oven at 105°C for about 10–20 h depending on the amount of roots. The drying can also be done at 60–75°C which will take longer but can have the advantage that this lower temperature prevents roots from being pulverized (Schuurman and Goedewaagen 1965).

Root weight is a good parameter for characterizing the total mass of roots in a soil. In all cases in which the productivity of underground terrestrial vegetation is to be determined, root dry weight should be the criterion for evaluation. This includes also all research in which the contribution of the roots for the amount of humus in the soil is to be studied. Root weight also can be regarded as a fundamental measure of photosynthate storage in a plant. The known shoot-root relations based mainly on shoot and root weight.

(3) Root surface
Surface area has seldom been determined in ecological research, although this parameter seems one of the best when experiments on water-or nutrient uptake are made. The most direct method is to determine the average diameter of a large number of individual roots and to measure the total root length per sample. From these data, root surface can be calculated easily (Geisler and Maarufi 1975; Adepetu and Akapa 1977). The main drawback to direct measurement is that the operator can decide only by inspection if the measured roots are still alive.

Wilde and Voigt (1949) proposed a method to determine the total root surface by titration. A simple method for determining relative root surface area is a gravimetric method developed by Carley and Watson (1966). Comparative studies made by Carley and Watson (1966) show that no significant differences in relative root surface areas exist between the titration method of Wilde and Voigt (1949) and this gravimetric method. The results obtained with the titration method have a higher accuracy, but the gravimetric method can be suitable in routine studies due to its greater speed and simplicity. A drawback of the gravimetric method is that fine roots can rope together and behave like thicker roots (Pearson 1974).

(4) Root volume
Root volume can be calculated by measuring root diameter and the root length. Such calculations, however, have seldom been done in practice. In general, for

measuring root volume, the water displacement technique is preferred. The measurement is done in a special container with an overflow spout. This container is filled with water until it overflows from the spout. Then fresh-washed roots which have been carefully dried with a soft cloth are immersed and the overflow water volume is measured in a graduated cylinder. The main reason for this limited use is certainly that root volume measurements from species with few large roots can be equal to species with large amounts of small fibrous roots. So the volume data alone are of limited value for most research problems in root ecology. Data from volumetric measurements in general should be used only to supplement other parameters.

(5) Root Diameter
In studies with annual plants, root diameter in most cases has been measured only for calculating root surface or root volume. But knowledge of the diameter of roots can give important information on the relationship between the pore size in a soil and the potential of root penetration (Wiersum 1957). The diameter is measured directly on freshly washed root samples with the aid of a microscope fitted with an ocular micrometer. Before starting the measurements, the roots are placed for some hours in water because many roots dry irregularly. Furthermore, it must be taken into account that there can be considerable diurnal variations in root diameter. On dry, sunny days, the diameter of roots can shrink to about 60% of its maximum size (Huck et al. 1970). Predominantly, in tree root studies, research workers confronted with the problem to differentiate between roots of various diameters. It is often convenient to divide roots into six classes with different root diameters in Table 3 (Böhm 1979). This classification must be regarded as arbitrary, and it would be wrong to identify root diameter with any particular kind of root function.

(6) Root Length
For direct measurements, the wet roots are placed in a flat glass dish containing a small amount of water. Graph paper is placed under the dish. The roots are straightened with forceps so that they do not overlap and are held in position by a glass plate. The lengths of the given roots or root segments are then estimated to the nearest millimeter by eye inspection or by the use of a magnifying glass. Obtaining root-length data by these direct measurements is tedious and time-consuming, and the procedure is recommended only for estimating the length of

Table 3 Classes of roots with different diameters

Root diameter (mm)	Classes of roots
<0.5	Very fine
0.5–2	Fine
2–5	Small
5–10	Medium
10–20	Large
>20	Very large

single root, not as a routine method in ecological research. Instead of tedious direct measurements, root length can be calculated more rapidly by counting the intersection method. The total number of intersections between the roots and the vertical and horizontal lines of a grid on the glass observation windows were counted. Comparisons of estimated intersection data with the measured actual root length show a linear relation between the number of intersections and the actual root length.

Independently of this practical line intersection method, Newman (1966) developed a theory that root length can be estimated by the Eq. (20):

$$R = \pi AN/2H \tag{20}$$

where R is the total length of roots in a field of area A and N are the number of intersections between the roots and random straight lines of total length H. Newman's method has been modified and improved by several research workers (Torssell et al. 1968; Evans 1970; Marsh 1971; Tennant 1975). The main change is that for the area over which the roots are spread, any convenient size of grid system can be used.

Practical tests done by Head (1966), Reicosky et al. (1970), and Tennant (1975) indicate that there are only small differences in the precision between the data from the direct measurements and those obtained from the intersection method. In no case has the standard deviation been more than $\pm 10\%$ of the true lengths, and in most cases, it has been much less.

(7) Root Tips
For determination, the cleaned roots are placed in a flat dish where they are kept under water. Here they are arranged so that they do not overlap. Then the number of live root tips is counted using a stereomicroscope. The distinction between live and dead root tips can be made by evaluating their morphology and color. Root tips are generally assumed to be alive if they are turgid, and white to light brown in color (Weller 1971). The main lamination seems to be that the counting procedure is very time-consuming and therefore not well adapted for routine studies.

(8) Shoot–Root Relations
The common parameter for evaluating the relations between above and below ground growth of plants is the shoot:root ratio. It is a measure of the distribution of dry weight between shoot and root system of the plants.

Many of the results of all this research indicate that the common assumption of a persistent tendency towards a positive correlation between shoots and roots are not generally valid. Ecological conditions can change the shoot:root ratio considerably when plants are growing under filed conditions. Nevertheless, studying shoot–root relations should be a central research filed for root ecologists. Adequate information is essential for analyzing or simulating growth pattern of whole plants (Mayaki et al. 1976; Sivakumar et al. 1977) and for

estimating primary productivity of ecosystems (Lieth and Whittaker 1975). However, when considering the efficiency of a root system for plant growth, root distribution in the soil profile, rather than total root weight, seems the more important factor.

With the development of technology, image analyses systems provide a quick determination of various root morphological parameters (root length, average diameter, surface area, and so on). Two image analyses programs using different measuring algorithms are often used, one is a commercial package WinRHIZO and the other is a freeware ROOTEDGE (Himmelbauer et al. 2004). ROOTEDGE is a computer program running under DOS and based on the edge chord algorithm (Ewing and Kaspar 1995). The program operates with binary (black-white) images in uncompressed tagged file (TIFF) format: root objects are assumed to be black and the background white. Root length, projected area, and average root diameter were determined. The commercial software package WinRHIZO 4.1 works under Windows and uses a skeletonization method for measuring the root parameters (Arsenault et al. 1995; Bauhus and Messier 1999; Smit et al. 1994). The program operates with 256 levels grayscale images in TIFF file format, which are further converted into threshold (binary) and skeleton images. Threshold images are used by the system for evaluation of root diameter, while root length is measured on the so-called skeleton images (Bauhus and Messier 1999). Measurements involved total root length, average root diameter, projected surface area, plus length and area measurements as a function of different root diameter classes. Additionally, the program detects overlapping parts and takes them into account when calculating root parameters.

Plant Root–Hydraulic Conductivity Relations

Soil Hydraulic Conductivity

A number of procedures have been developed for estimating soil hydraulic conductivity from tension infiltrometer data. These include methods by White and Perroux (1989), Smettem and Clothier (1989), and Reynolds and Elrick (1991). These methods vary greatly in their capabilities, procedures, assumptions, and complexity. The procedure developed by Reynolds and Elrick (1991) have been widely used (Yu et al. 2016). According to Reynolds and Elrick (1991), the soil hydraulic conductivity (K_h) was given:

$$K(h)=K_s \exp(\alpha^* h) \tag{21}$$

h is the pressure head (cm), K_s is the saturated hydraulic conductivity (cm h^{-1}), and α (cm^{-1}) is the sorptive number. So the K_s can be calculated by the Gardner's exponential model (Gardner 1958). Parameters (K_s and α) were obtained by fitting the function of $K(h)$ to the measured K_h vs. h data pairs using a nonlinear fitting procedure with a Levenberg Marquardt optimization algorithm.

For the different species and positions, the soil hydraulic conductivity at different supply pressure heads measured by tension infiltrometry are different. Table 4 shows

Table 4 Soil hydraulic conductivity (Kh) at different pressure heads (h = −15, −10, −3, −1 cm) measured by tension infiltrometry (Yu et al. 2016)

	K_{15} (cm h^{-1})		K_{10} (cm h^{-1})		K_3 (cm h^{-1})		K_1 (cm h^{-1})	
Species	Row	Interrow	Row	Interrow	Row	Interrow	Row	Interrow
V. sativa	0.24	0.22	0.39	0.40	4.26	2.98	13.13	9.24
Mixture 1	0.15	0.05	0.27	0.19	2.46	2.13	7.46	5.94
M. officinalis	0.19	0.17	0.40	0.26	5.60	1.45	23.36	3.02
L. sativus	0.31	0.21	0.60	0.37	5.73	2.46	20.32	6.18
Mixture 2	0.26	0.16	0.49	0.28	4.47	1.87	15.32	3.94
T. lexandrinum	0.32	0.23	0.64	0.39	5.23	2.2	14.36	4.78
S. alba	0.30	0.24	0.52	0.43	1.99	2.72	3.16	6.28
F. esculentum	0.29	0.23	0.51	0.40	4.00	2.15	10.66	4.50
L. sitatissimum	0.33	0.24	0.64	0.41	5.29	3.03	15.08	8.38
P. tanacetifolia	0.24	0.21	0.48	0.40	3.48	3.62	8.46	10.42
R. sativus	0.20	0.20	0.38	0.34	3.44	2.27	11.35	5.73
S. cereale	0.26	0.19	0.47	0.33	4.15	2.69	12.25	7.37

the soil hydraulic conductivity at different supply pressure heads measured by tension infiltrometry for the different species and positions in Australia (Yu et al. 2016). Statistical analysis revealed a significant interaction between species and position ($p < 0.001$). Species clusters for the row and interrow position was given in Fig. 28 (Yu et al. 2016).

Species with significantly higher K_h in the row compared to the interrow were *Melilotus officinalis*, *L. sativus*, Mixture 2, *Trifolium alexandrinum*, *L. usitatissimum,* and *Secale cereale*. Among the species, the differentiation in K_h was higher in the row (CV = 0.37) compared to the interrow (CV = 0.30). In the row, the legumes as well as *L. usitatissimum* commonly induced an average high K_h, while the brassicas together with *S. cereale* and Mixture 1 had low values. In the interrow, there was no evident distinction in K_h between plant families. Some legume species with high K_h in the row had a rather low value in the interrow such as *M. officinalis* or *T. alexandrinum* as well as the legume based Mixture 2. In the interrow, *Phacelia tanacetifolia* and *V. sativa* had the highest K_h, while *L. usitatissimum* showed high K_h in both the row and interrow.

The two parameters of the exponential Gardner model to describe the entire K_h curve are derived and shown in Table 5. Both parameters showed a significant interaction of species × position and had higher values in the row than in the interrow. Among species, *V. sativa*, *M. officinalis,* and *L. sativus* had both very high K_s and α values, while *Sinapis alba* and Mixture 1 were at the lower end in both parameters. For *Raphanus sativus,* the value of α was in very low range, while they had an intermediate K_s.

Plant Root–Hydraulic Conductivity Relations

Based on the parameters characterizing the root systems and the soil hydraulic conductivity function, which root trait provides the best predictor for hydraulic

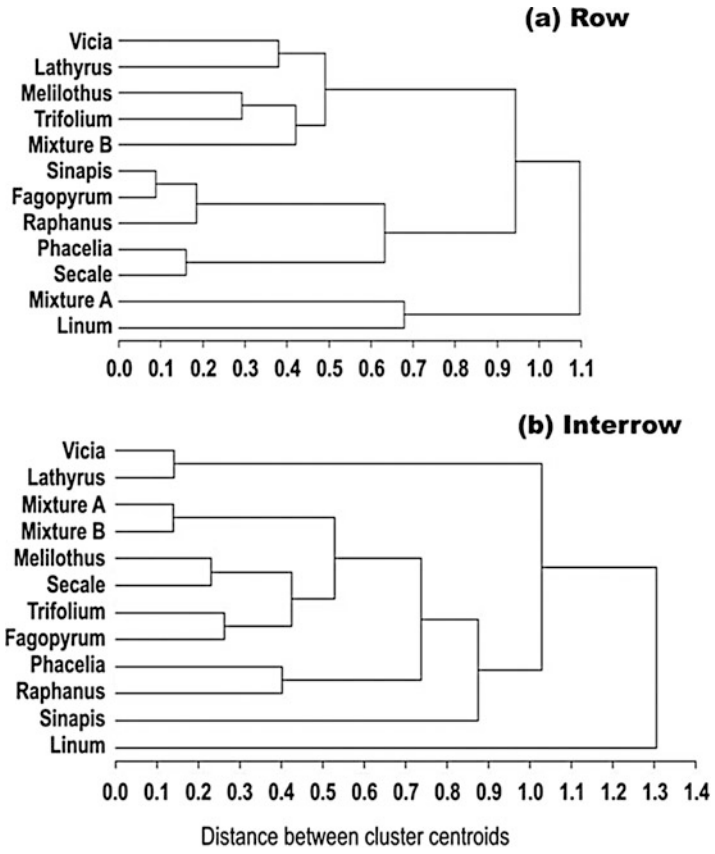

Fig. 28 Dendrogramm showing similar root system types among cover crop species based on the cluster analysis using root traits for row (**a**) and interrow (**b**) (Yu et al. 2016)

conductivity was analyzed by Yu et al. (2016). As shown in Fig. 29, in the row, specific root length (SRL) was the best root predictor for K_s and α, being negatively related to both parameters, i.e., species with a predominant root biomass investment in coarse root length enhanced saturated hydraulic conductivity while showing a quick decrease of the K_h function toward lower pressure heads. In the interrow, the best root predictor for the Gardner parameters was the median root radius (MRR). Interestingly, at this position, MRR showed a negative relation to the hydraulic conductivity descriptors, i.e., species with their root volume allocated to coarser axes here tended to reduce K_s while showing a lower decrease of K_h toward smaller pores. The coarse root might enlarge the soil porosity and a non-Darcy behavior (The relationship between infiltration rate and head loss rate is not proportional.) occurs.

Table 5 Parameters of Gardner's soil hydraulic conductivity function (*Ks* is saturated hydraulic conductivity, α is the sorptive number) as influenced by cover crop species and measurement position (row vs. interrow) (Yu et al. 2016)

	K_s (cm h^{-1})	α (cm^{-1})
Species (S)	0.160	0.111
Position (P)	<0.001	<0.001
S _ P	0.037	0.004
Position		
Row	23.22	0.49
Interrow	10.08	0.26
s.e.d.	2.55	0.02
Species		
V. sativa	19.93	0.40
Mixture 1	11.91	0.30
M. officinalis	25.72	0.45
L. sativus	24.82	0.42
Mixture 2	17.66	0.41
T. alexandrinum	15.43	0.41
S. alba	6.71	0.25
F. esculentum	11.92	0.38
L. usitatissimum	19.19	0.41
P. tanacetifolia	14.84	0.34
R. sativus	15.14	0.35
S. cereale	16.57	0.39
s.e.d.	5.97	0.07

Root Impact on Surface Runoff Mitigation

The changes in soil hydraulic conductivity driven by morphologically different root systems of cover crops have a significant impact on surface runoff. Yu et al. (2016) analyzed the potential impact of root-induced modifications of soil hydraulic conductivity on surface runoff, which was estimated by HYDRUS 2D. Figure 30 shows the soil hydraulic property parameters calculated to run the HYDRUS simulation. The Gardner exponential model estimates higher K_h values in the wet range while decreasing quickly toward the dry range. The Mualem–Van Genuchten hydraulic conductivity function on the contrary quickly falls below the saturated conductivity while the function then decreases more smoothly toward lower pressure heads. The cross-over between the average hydraulic conductivity functions based on K_s and Gardner's vs. Mualem–Van Genuchten's α is at a pressure head value of about $h = 0.1$ m. Below this cross-over point ($h = 0.1$ m), the tension infiltrometer measurement points in the near-saturated range are nearer to the Mualem–Van Genuchten function, while the tension infiltrometer measurement points in the near-saturated range are in better agreement with the Gardner model at higher pressure heads.

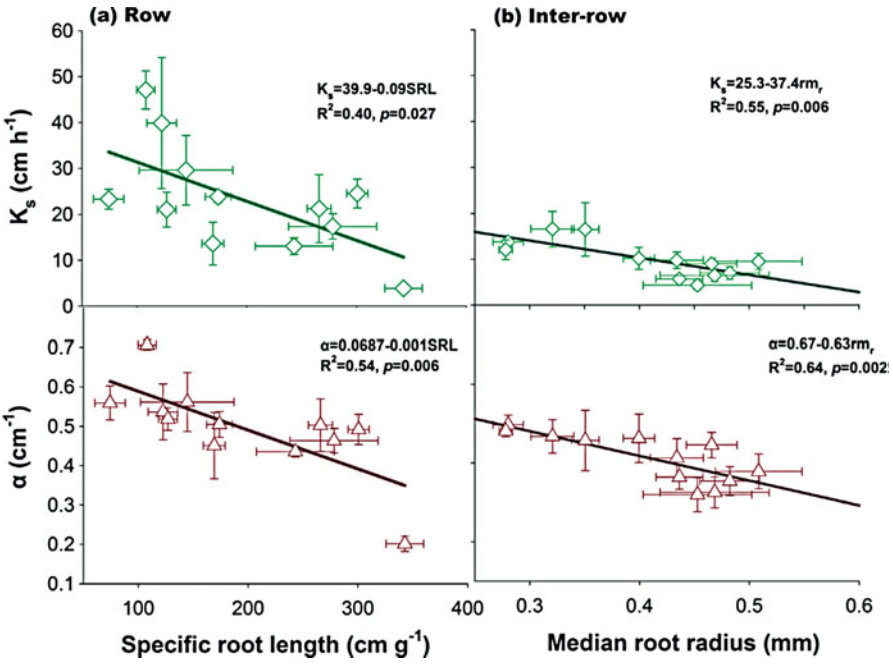

Fig. 29 Relationships between best root predictor and parameters of Gardner's exponential soil hydraulic conductivity function (**a**) in the row and (**b**) in the interrow (Yu et al. 2016)

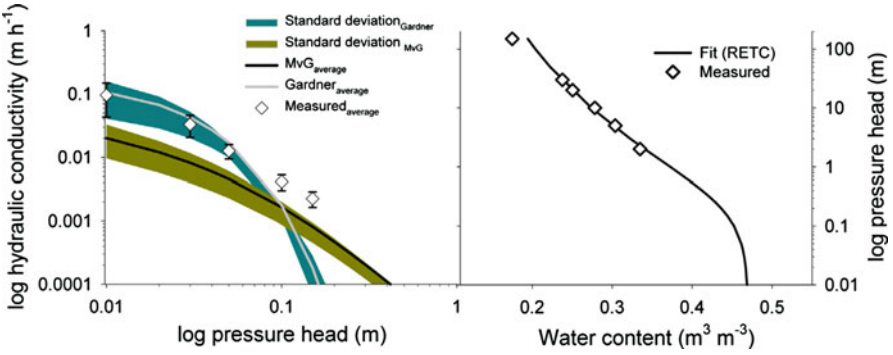

Fig. 30 Soil hydraulic functions used for runoff simulation with HYDRUS 2D. Left figure: Example of a representative hydraulic conductivity curve (mean of all measurements and standard deviation) using the Gardner and Mualem–Van Genuchten functions compared to point measurements. Right figure: Van Genuchten retention curve estimated from pressure plate data using RETC (Yu et al. 2016)

Figure 31 shows the runoff simulation result estimated by HYDRUS 2D when using the distinct row and interrow hydraulic properties corresponding to the different cover crop species. In each scenario, the cumulative rainfall was 20 mm over 72 h, with scenario 1 representing high intensity rainfall (intensity = 20 mm h^{-1}) on a dry soil,

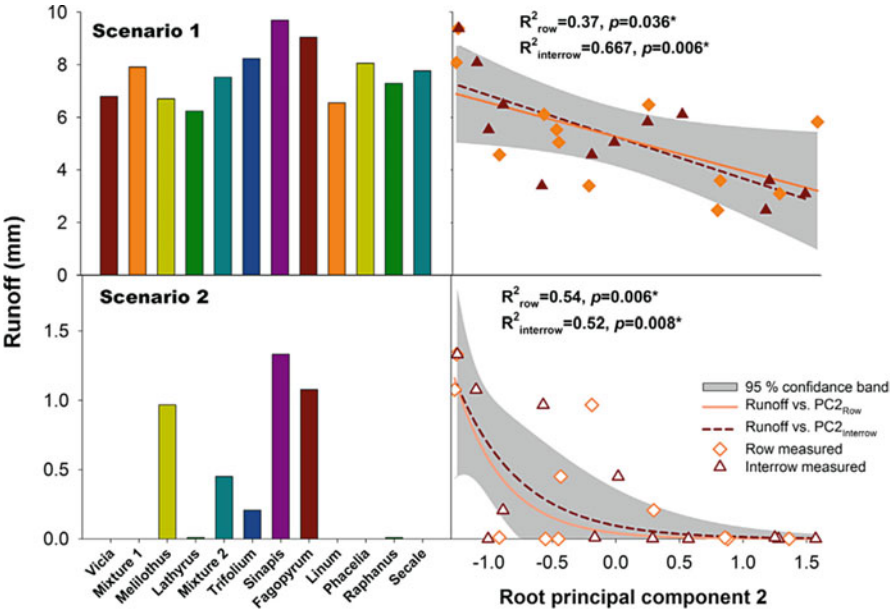

Fig. 31 Simulated runoff for different cover crops and two rainfall scenarios (left), relation between runoff and best root predictor (right). The root principal component 2 is a multivariate descriptor for axes thickness containing root diameter, specific root length, and median root radius. Scenario 1 represents a short, high intensity rainfall on initially dry soil; scenario 2 simulates rainfall over longer duration with low intensity on initially wet soil. In both scenarios, the cumulative rainfall amount is 20 mm (Yu et al. 2016)

while scenario 2 was a more extended rainfall (maximum intensity = 5 mm h^{-1}) on an initially wet soil. As expected, the intense rainfall scenario resulted in higher runoff losses and for all species, while under reduced rainfall intensity, soil infiltrability under most cover crops was high enough to take up all incoming precipitations. The low hydraulic conductivity of soil planted with *S. alba* showed highest runoff with nearly 50% of total rainfall lost. *L. sativus* on the contrary exhibited the lowest runoff losses with only 31% of incoming rainfall. In case of high intensity rainfall, the root effect on K_s is predominant explaining 79% of variability in the estimated amount of runoff. If root principal component 2 (The root principal component 2 is a multivariate descriptor for axes thickness containing root diameter, specific root length, and median root radius.) as a comprehensive descriptor of traits related to root axes thickness (SRL, MRR, RV) with a positive value describing root systems with high root volume of predominantly coarse axes was used, the amount of runoff was reduced by such rooting types which is expressed by the average lower runoff under legumes. However, the surface runoff of *L. usitatissimum* with a highly dense root system is efficiently mitigated. Under less intensive rainfall, only five species had runoff higher 1% of incoming rainfall

with peak values for *S. alba*, *Fagopyrum esculentum,* and *M. officinalis*. Here the limiting factor appeared to be related to a instead of K_s, where the interrow showed the strongest relation ($R^2 = 0.60$, $p = 0.03$) with higher α values constraining infiltrability. The relation to root axes thickness expressed by the composite principal component descriptor was similar to the high intensity scenario but following an exponential trend.

Outlooks

The runoff generation and flow concentration are the vital processes of terrestrial ecosystem during the water cycles. This process includes the water movement in the soil, the subsurface runoff, slope surface runoff, and the runoff generation in watershed. The formation of surface runoff is complex and highly variable on spatial and temporal scales, which is always the root of uncertainty and the theoretical bottleneck of hydrological analysis and accurate predictions as well as simulations.

1. To explore the impact of vegetation on the mechanism of surface runoff formation, it is necessary to carry out the in situ observations of runoff process on slope and watershed scales, respectively under different vegetation conditions. So far, such observations have only been done in typical vegetation basins, which lead to the ambiguous mechanism of runoff formation on basin or regional scales. Therefore, the establishment of surface runoff observation network in different ecological system is not only the ultimate approach to further understanding of mechanism of surface runoff formation but also a basis for constructions of high precision hydrological models.
2. The development of distributed hydrological models based on physical mechanism, to some extent, has played an important role in the accurate simulation of surface runoff. However, it is undeniable that the data processing of ecological factors tends to be simple, taking a common case of vegetation to be parameterized as input in most of the models without any consideration to apply merits of land surface process models into hydrological models. Therefore, the combination of land surface model and distributed hydrological model will greatly improve the accuracy and effectiveness of simulation results. This is also the main developing direction of watershed hydrological models in the future.
3. For the ecological process, most of the studies can be based on individual organisms, community, or transect. However, most of the surface runoff processes were identified based on the scales of sample plots, slope, catchment area, or small watershed. Therefore, the slope surface, water catchment unit, or subbasin become the ideal scales to link ecology and hydrology. However, how to integrate the ecological process and the runoff process on different scales or on larger scale (such as watershed or regional scale)? How to couple the surface runoff process and the ecological process under the background climate change?

The lack of the feasible observation technique and simulation method has become the obstacles on the way and also one of the greatest challenges for the development and application of eco-hydrology.

Acknowledgments This research was financially supported by the National Natural Science Foundation of China (41430748 and 41661144025).

References

M.B. Abbott, J.C. Bathurst, J.A. Cunge, P.E. O'Connell, J. Rasmussen, An introduction to the European Hydrological System – Systeme Hydrologique Europeen, "SHE", 1: history and philosophy of a physically-based, distributed modelling system. J. Hydrol. **87**(1), 45–59 (1986)

J.R.C.B. Abrantes, R.B. Moruzzi, A. Silveira, J.L.M.P.D. Lima, Comparison of thermal, salt and dye tracing to estimate shallow flow velocities: novel triple-tracer approach. J. Hydrol. **557**, 362–377 (2018)

J.A. Adepetu, L.K. Akapa, Root growth and nutrient uptake characteristics of some cowpea varieties. Agron. J. **69**(6), 940–943 (1977)

O. Al-Jubeh, Studies of natural vegetation characteristics at different Environment and range improvement practices at southern West Bank, M. Sc thesis, Hebron University, 2006

G.F. Antonious, Reducing herbicide residues from agricultural runoff and seepage water. (2015)

J.L. Arsenault, S. Poulcur, C. Messier, R. Guay, WinRHlZO™, a root-measuring system with a unique overlap correction method. Hortscience Am. Soc. Horticult. Sci. **30**(4), 906 (1995)

C. Asdak, P.G. Jarvis, P.V. Gardingen, A. Fraser, Rainfall interception loss in unlogged and logged forest areas of Central Kalimantan, Indonesia. J. Hydrol. **206**(3), 237–244 (1998)

S.D. Baets, J. Poesen, B. Reubens, K. Wemans, J.D. Baerdemaeker, B. Muys, Root tensile strength and root distribution of typical Mediterranean plant species and their contribution to soil shear strength. Plant Soil **305**(1–2), 207–226 (2008)

D.H. Barker, *Vegetation and Slopes: Stabilization, Protection and Ecology* (Thomas Telford, London, 1995)

J. Bauhus, C. Messier, Evaluation of fine root length and diameter measurements obtained using RHIZO image analysis. Agron. J. **91**(1), 142–147 (1999)

A.G. Bengough, Water dynamics of the root zone: rhizosphere biophysics and its control on soil hydrology. Vadose Zone J. **11**(2), 460–460 (2012)

S. Bergstrom, *Computer Models of Watershed Hydrology*. (1995), pp. 443–476

K.J. Beven, M.J. Kirkby, Taylor & Francis Online: A physically based, variable contributing area model of basin hydrology/Un modèle à base physique de zone d'appel variable de l'hydrologie du bassin versant. Hydrol. Sci. Bull. **24**(1), 43–69 (1979)

E.W. Bhark, E.E. Small, Association between plant canopies and the spatial patterns of infiltration in shrubland and grassland of the Chihuahuan Desert, New Mexico. Ecosystems **6**(2), 0185–0196 (2003)

G. Bodner, L. Daniel, N. Alireza, S. Monika, M. Karl, K. Hans-Peter, A statistical approach to root system classification. Front. Plant Sci. **4**(4), 292–292 (2013)

W. Böhm, *Methods of Studying Root Systems* (Springer, Berlin/Heidelberg/New York, 1979), pp. 1–3

W. Boughton, A hydrograph-based model for estimating the water yield of ungauged catchments. Proc. Hydrol. Water Resour. Symp. Newcastle Inst. Engs. Aust. Nat. Conf. Publ. **93**(14), 317–324 (1993)

W. Boughton, F. Chiew, Calibrations of the AWBM for use on ungauged catchments. Am. Soc. Civ. Eng. **14**(6), 562–568 (2003)

D.L. Brakensiek, H.B. Osborn, W.J. Rawls, *Field Manual for Research in Agricultural Hydrology*. (1979)

F. Branson, G. Gifford, J. Owen, Rangeland hydrology. Range Science Series No. 1, Soc. Range Manage., Denver CO. (1972)

F. Branson, G. Gifford, K. Renard, R. Hadley, Rangeland Hydrology. Range Sciences Series No. 1, October 1972, 1981. Soc. Range Manage., Denver CO. Kendall (ed.), (Hunt Publishing Co., Dubuque, 1981)

J. Bromley, J. Brouwer, A. Barker, S. Gaze, C. Valentine, The role of surface water redistribution in an area of patterned vegetation in a semi-arid environment, south-west Niger. J. Hydrol. **198**, 1–29 (1997)

C.J. Bronick, R. Lal, Soil structure and management: a review. Geoderma **124**(1–2), 3–22 (2005)

P. Burlando, Hydrograph separation of runoff components based on measuring hydraulic state variables, tracer experiments, and weighting methods. Paper presented at integrated methods in catchment hydrology: tracer, remote sensing and new hydrometric techniques: proceedings of an international symposium held during IUGG 99, the XXII General Assembly of the International Union of Geodesy and Geophysics, Birmingham, IAHS, 18–30 July 1999

R.J.C. Burnash, R.L. Ferral, R.A. Mcguire, *A generalized streamflow simulation system – conceptual modeling for digital computers*. (1973)

J.M. Buttle, Isotope hydrograph separations and rapid delivery of pre-event water from drainage basins. Prog. Phys. Geogr. **18**(1), 16–41 (1994)

J.M. Buttle, in *Chapter 1 – Fundamentals of Small Catchment Hydrology*, Isotope Tracers in Catchment Hydrology (1998)

I.R. Calder, P.T.W. Rosier, The design of large plastic-sheet net-rainfall gauges. J. Hydrol. **30**(4), 403–405 (1976)

A. Calver, W.L. Wood, V.P. Singh, The Institute of Hydrology distributed model (1987)

Y. Cantón, A. Solébenet, V.J. De, C. Boixfayos, A. Calvocases, C. Asensio, J. Puigdefábregas, A review of runoff generation and soil erosion across scales in semiarid south-eastern Spain. J. Arid Environ. **75**(12), 1254–1261 (2011)

H.E. Carley, R.D. Watson, A new gravimetric method for estimating root-surface areas. Soil Sci. **102**(5), 289–291 (1966)

D.E. Carlyle-Moses, J.S.F. Laureano, A.G. Price, Throughfall and throughfall spatial variability in Madrean oak forest communities of northeastern Mexico. J. Hydrol. **297**(1–4), 124–135 (2004)

C.E. Carter, D.A. Parsons, Field tests on the Coshocton-type wheel runoff sampler, 0133–0135 (1967)

A. Cerda, Parent material and vegetation affect soil erosion in eastern Spain. Soil Sci. Soc. Am. J. **63**(2), 362–368 (1999)

V.A. Chaplot, Y. Le Bissonnais, Runoff features for interrill erosion at different rainfall intensities, slope lengths, and gradients in an agricultural loessial hillslope. Soil Sci. Soc. Am. J. **67**(3), 844–851 (2003)

F.H.S. Chiew, M.C. Peel, A.W. Western, V.P. Singh, D. Frevert, Application and testing of the simple rainfall-runoff model. SIMHYD, 335–367 (2002)

S.K. Chong, R.E. Green, Sorptivity measurement and its application. (1983)

C.A.A. Ciesiolka, B. Yu, C.W. Rose, H. Ghadiri, D. Lang, C. Rosewell, Improvement in soil loss estimation in USLE type experiments. J. Soil Water Conserv. **61**(4), 223–229 (2006)

E.A. Colman, Vegetation and watershed management (1953)

E.S. Corbett, Rainfall interception by annual grass and chaparral; losses compared (1968)

N.H. Crawford, The synthesis of continuous streamflow hydrographs on a digital computer (1962)

N.H. Crawford, R.E. Linsley, Digital simulation in hydrology: Stanford watershed model IV, Evapotranspiration, 39 (1966)

H.P. Cresswell, J.A. Kirkegaard, Subsoil amelioration by plant-roots – the process and the evidence. Soil Res. **33**(2), 221–239 (1995)

H.P. Creswell, D.E. Smiles, J. Williams, Soil structure, soil hydraulic properties and the soil water balance. Aust. J. Soil Res. **30**(3), 265–283 (1992)

R.H. Crockford, D.P. Richardson, Partitioning of rainfall into throughfall, stemflow and interception: effect of forest type, ground cover and climate. Hydrol. Process. **14**(16–17), 2903–2920 (2000)

Y. Cui, L. Jia, A modified Gash model for estimating rainfall interception loss of forest using remote sensing observations at regional scale. Water **6**(4), 993–1012 (2014)

M.S. Czarnowski, J.L. Olszewski, Number and spacing of rainfall-gauges in a deciduous forest stand. Oikos **21**(1), 48–51 (1970)

A.P.J. De Roo, R.J.E. Offermans, N.H.D.T. Cremers, LISEM: a single-event, physically based hydrological and soil erosion model for drainage basins. II: sensitivity analysis, validation and application. Hydrol. Process. **10**(8), 1119–1126 (2015)
C. Deasy, J.N. Quinton, M. Silgram, A.P. Bailey, B. Jackson, C.J. Stevens, Mitigation options for sediment and phosphorus loss from winter-sown Arable Crops. J. Environ. Qual. **38**(38), 2121–2130 (2009)
S.L. Dingman, Physical hydrology. Phys. Hydrol. **11**(1), 112–120 (2002)
M. Dohnal, T. Černý, J. Votrubová, M. Tesař, Rainfall interception and spatial variability of throughfall in spruce stand. J. Hydrol. Hydromech. **62**(4), 277–284 (2014)
M.G. Dosskey, K.D. Hoagland, J.R. Brandle, Change in filter strip performance over ten years. J. Soil Water Conserv. **62**(1), 21–32 (2007)
F. Duley, C.E. Domingo, Effect of grass on intake of water (1949)
G. Dunjó, G. Pardini, M. Gispert, The role of land use–land cover on runoff generation and sediment yield at a microplot scale, in a small Mediterranean catchment. J. Arid Environ. **57**(2), 239–256 (2004)
D. Dunkerley, Hydrologic effects of dryland shrubs: defining the spatial extent of modified soil water uptake rates at an Australian desert site. J. Arid Environ. **45**(2), 159–172 (2000)
T. Dunne, Field studies of hillslope flow processes, in *Hillslope Hydrology*, ed. by M. J. Kirkby (Ed), (Wiley, New York, 1978), pp. 227–293
T. Dunne, W.E. Dietrich, Experimental study of Horton overland flow on tropical hillslopes; 1, Soil conditions, infiltration and frequency of runoff. Z. Geomorphol. **2**, 40–80 (1980)
T. Dunne, T.R. Moore, C.H. Taylor, Recognition and prediction of runoff-producing zones in humid regions. Hydrol. Sci. Bull, 20, 305–327 (1975)
T. Dunne, W. Zhang, B.F. Aubry, Effects of rainfall, vegetation, and microtopography on infiltration and runoff. Water Resour. Res. **27**(9), 2271–2285 (1991)
J. Dusek, T. Vogel, M. Dohnal, H.H. Gerke, Combining dual-continuum approach with diffusion wave model to include a preferential flow component in hillslope scale modeling of shallow subsurface runoff. Adv. Water Resour. **44**(44), 113–125 (2012)
E. Dyksterhuis, E. Schmutz, Natural mulches or "litter" of grasslands: with kinds and amounts on a southern prairie. Ecology **28**(2), 163–179 (1947)
I.J. Edwards, W.D. Jackon, P.M. Fleming, Tipping bucket gauges for measuring run-off from experimental plots. Agric. Meteorol. **13**(2), 189–201 (1974)
M. Eshghizadeh, A. Talebi, M.T. Dastorani, H. Azimzadeh, Effect of natural land covers on runoff and soil loss at the hill-slope scale. Glob. J. Environ. Sci. Manag. **2**, 125–134 (2015)
P.S. Evans, Root growth of Lolium perenne L. 1. Effect of plant age, seed weight, and nutrient concentration on root weight, length and number of apices. N. Z. J. Bot. **8**, 544–556 (1970)
R.P. Ewing, T.C. Kaspar, Accurate perimeter and length measurement using an edge chord algorithm. J. Comput.-Assist. Microsc. **7**, 91–100 (1995)
D.X. Fan, Study on slope soil erosion response and model simulation in Beijing mountainous area, 166 (2014)
Y. Fan, R.L. Bras, Analytical solutions to hillslope subsurface storm flow and saturation overland flow. Water Resour. Res. **34**(4), 921–928 (1998)
J. Fan, K.T. Oestergaard, A. Guyot, D.A. Lockington, Measuring and modeling rainfall interception losses by a native Banksia woodland and an exotic pine plantation in subtropical coastal Australia. J. Hydrol. **515**(13), 156–165 (2014)
A.D. Feldman, Hec models for water resources system simulation: theory and experience. Adv. Hydrosci. **12**, 297–423 (1981)
D. Flanagan, M. Nearing, USDA-Water Erosion Prediction Project: hillslope profile and watershed model documentationRep., NSERL report (1995)
J.P. Fortin, R. Turcotte, S. Massicotte, R. Moussa, J. Fitzback, J.P. Villeneuve, Distributed watershed model compatible with remote sensing and GIS data. II: application to Chaudière watershed. J. Hydrol. Eng. **6**(2), 91–99 (2001)

C. Francis, J. Thornes, Runoff hydrographs from three Mediterranean vegetation cover types, vegetation and erosion. Process. Environ., 363–384 (1990)
Z. Gan, J. Ye, Q. Zhou, Z. Zhou, Z. Shangguan, Effects of grass vegetations on the processes of soil erosion over slope lands in simulated rainfalls. Acta Ecol. Sin. **30**(9), 2387–2396 (2010)
W.R. Gardner, Some steady-state solutions of the unsaturated moisture flow equation with application to evaporation from a water table. Soil Sci. **85**(4), 228–232 (1958)
J. Gash, An analytical model of rainfall interception by forests. Q. J. R. Meteorol. Soc. **105**(443), 43–55 (1979)
M.J. Gavazzi, G. Sun, S.G. McNulty, E.A. Treasure, M.G. Wightman, Canopy rainfall interception measured over ten years in a coastal plain loblolly pine (Pinus taeda L.) plantation. Trans. ASABE **59**(2), 601–610 (2016)
G. Geisler, D. Maarufi, Investigations on the importance of the root systems of cultivated plants, 1: the influence of the soil water content and nitrogen manuring on plant growth, root morphology, transpiration and nitrogen absorption (1975)
S. Germer, L. Werther, H. Elsenbeer, Have we underestimated stemflow? Lessons from an open tropical rainforest. J. Hydrol. **395**(3–4), 169–179 (2010)
M. Ghestem, R.C. Sidle, A. Stokes, The influence of plant root systems on subsurface flow: implications for slope stability. Bioscience **61**(11), 869–879 (2011)
W.H. Green, G. Ampt, Studies on soil phsyics. J. Agric. Sci. **4**(1), 1–24 (1911)
J.H. Gregory, M.D. Dukes, G.L. Miller, P.H. Jones, Analysis of double-ring infiltration techniques and development of a simple automatic water delivery system, Appl. Turfgrass Sci., 2 (2005)
G. Gyssels, J. Poesen, E. Bochet, Y. Li, Impact of plant roots on the resistance of soils to erosion by water: a review. Prog. Phys. Geogr. **29**(2), 189–217 (2005)
A. Hanchi, M. Rapp, Stemflow determination in forest stands. For. Ecol. Manag. **97**(3), 231–235 (1997)
D.M. Harris, J.J. Mcdonnell, A. Rodhe, Hydrograph separation using continuous open system isotope mixing. Water Resour. Res. **31**(1), 157–171 (1995)
R.J. Haynes, M.H. Beare, Influence of six crop species on aggregate stability and some labile organic matter fractions. Soil Biol. Biochem. **29**(11), 1647–1653 (1997)
G.C. Head, Estimating seasonal changes in the quantity of white unsuberized root on fruit trees. J Pomol Hortic Sci **41**(2), 197–206 (1966)
J. Helvey, J.H. Patric, Canopy and litter interception of rainfall by hardwoods of eastern United States. Water Resour. Res. **1**(2), 193–206 (1965)
M. Herbst, J.M. Roberts, P.T.W. Rosier, D.J. Gowing, Measuring and modelling the rainfall interception loss by hedgerows in southern England. Agric. For. Meteorol. **141**(2–4), 244–256 (2006)
A.G.J. Hilberts, P.A. Troch, C. Paniconi, J. Boll, Low-dimensional modeling of hillslope subsurface flow: Relationship between rainfall, recharge, and unsaturated storage dynamics. Water Resour. Res. **43**(3), 305–310 (2007)
L.M. Himmelbauer, Loiskandl, Kastanek, Estimating length, average diameter and surface area of roots using two different image analyses systems: new challenges for rhizosphere research at the entrance of the 21st century. Plant Soil (2004)
H.N. Holtan, Concept for infiltration estimates in watershed engineering (1961)
F. Holwerda, F.N. Scatena, L.A. Bruijnzeel, Throughfall in a Puerto Rican lower montane rain forest: a comparison of sampling strategies. J. Hydrol. **327**(3), 592–602 (2006)
R. Horn, A. Smucker, Structure formation and its consequences for gas and water transport in unsaturated arable and forest soils. Soil Tillage Res. **82**(1), 5–14 (2005)
R.E. Horton, Rainfall interception. Mon. Weather Rev. **47**(9), 603–623 (1919)
R.E. Horton, An approach toward a physical interpretation of infiltration-capacity. Soil Sci. Soc. Am. J. **5**(C), 399–417 (1941)
R. Horton, R. Horton, R.R. Horton, R.E. Horton, R. Horton, R.E. Horton, An approach towards physical interpretation of infiltration capacity (1940)

M. Hrnčíř, M. Šanda, A. Kulasová, M. Císlerová, Runoff formation in a small catchment at hillslope and catchment scales. Hydrol. Process. **24**(16), 2248–2256 (2010)
S.P. Hu, Y.U. Xinxiao, Y.U.E. Yongjie, Hydrological effects of forest litters and soil in Baihua Mountain. J. Soil Water Conserv. **22**(1), 146–150 (2008)
P. Hubert, E. Marin, M. Meybeck, P. Olive, E. Siwertz, Aspects Hydrologiques et Sedimentologigues de la Crue Exceptionnelle de la Dranse du Chablais du 22 Septembre 1968 (1969)
M.G. Huck, B. Klepper, H.M. Taylor, Diurnal variations in root diameter. Plant Physiol. **45**(4), 529 (1970)
N. Hudson, Field measurement of soil erosion and runoff, Food & Agriculture Org (1993)
T. Iserloh, J.B. Ries, J. Arnáez, C. Boix-Fayos, V. Butzen, A. Cerdà, M.T. Echeverría, J. Fernández-Gálvez, W. Fister, C. Geißler, European small portable rainfall simulators: a comparison of rainfall characteristics. Catena **110**(11), 100–112 (2013a)
T. Iserloh, J.B. Ries, A. Cerdà, M.T. Echeverría, W. Fister, C. Geißler, N.J. Kuhn, F.J. León, P. Peters, M. Schindewolf, Comparative measurements with seven rainfall simulators on uniform bare fallow land. Z. Geomorphol. **57**(3), 11–26 (2013b)
A.J. Jakeman, G.M. Hornberger, How much complexity is warranted in a rainfall-runoff model? Water Resour. Res. **29**(8), 2637–2649 (1993)
C. Johnson, N. Gordon, Runoff and erosion from rainfall simulator plots on sagebrush rangeland. Trans. ASAE **31**(2), 421–427 (1988)
W. Johnson, C. Niederhof, Some relationships of plant cover to run-off, erosion, and infiltration on granitic soils. J. For. **39**(10), 854–858 (1941)
T.J. Ju, L.I.U. Puling, X.U. Xuexuan, W. Shuanquan, S.H.I. Xinhe, Experimental study on runoff and sediment process in primary-lands in loess hilly regions under different rainfall conditions. J. Sediment Res. **4**, 65–71 (2007)
Y. Kavdır, A.J.M. Smucker, Soil aggregate sequestration of cover crop root and shoot-derived nitrogen. Plant Soil **272**(1–2), 263–276 (2005)
A.A.H. Khan, C.K. Ong, Design and calibration of tipping bucket system for field runoff and sediment quantification. Paper presented at J. Soil Water Conserv. (1997)
P.I.A. Kinnell, The effect of kinetic-energy of excess rainfall on soil loss from non-vegetated plots. Aust. J. Soil Res. **21**(4), 445–453 (1983)
P. Kinnell, The IXEA index: an index with the capacity to give more direct consideration of hydrology in the USLE modelling environment. J. Soil Water Conserv. **50**, 507–512 (1995)
P.I.A. Kinnell, A review of the design and operation of runoff and soil loss plots. Catena **145**, 257–265 (2016)
Kinnell, P. I. A., K. C. Mcgregor, and C. J. Rosewell (1994), The IXEA index as an alternative to the El30 erosivity index, 37(5), 1449-1456.
G. Kite, in *The SLURP Model*, ed. By Singh. Computer Models of Watershed Hydrology (1995)
A.N. Kostiakov, On the dynamics of the coefficient of water-percolation in soils and on the necessity of studying it from a dynamic point of view for purposes of amelioration, Trans. 6th Cong. International. Soil Science, Russian Part A, 17–21 (1932)
B. Kothyari, P. Verma, B. Joshi, U. Kothyari, Rainfall–runoff-soil and nutrient loss relationships for plot size areas of Bhetagad watershed in Central Himalaya, India. J. Hydrol. **293**(1), 137–150 (2004)
N. Kouwen, S.F. Mousavi, V.P. Singh, D.K. Frevert, WATFLOOD/SPL9 hydrological model & flood forecasting system. Mathematical Models of Large Watershed Hydrology (2002)
N.J. Kuhn, P. Greenwood, W. Fister, Use of field experiments in soil erosion research, 175–200 (2014)
R. Lei, Effect of a larix principis-rupprechtii forestplantation on soil in middle zone of south-facingslope of the Qinling mountains. Sci Silvae Sin. (1997)
T. Lei, W. Xia, J. Zhao, Z. Liu, Q. Zhang, Method for measuring velocity of shallow water flow for soil erosion with an electrolyte tracer. J. Hydrol. **301**(1–4), 139–145 (2005)
T.W. Lei, C. Ruiyuan, J. Zhao, X.N. Shi, L. Lin, An improved method for shallow water flow velocity measurement with practical electrolyte inputs. J. Hydrol. **390**(1–2), 45–56 (2010)

J. Leonard, P. Andrieux, Infiltration characteristics of soils in Mediterranean vineyards in Southern France. Catena **32**(3), 209–223 (1998)
D.F. Levia, E.E. Frost, A review and evaluation of stemflow literature in the hydrologic and biogeochemical cycles of forested and agricultural ecosystems. (Elsevier B.V., 2003), pp. 1–29
Y. Li, X. Xu, X. Zhu, Preliminary-study on mechanism of plant-roots to increase soil anti-scouribility on the Loess Plateau. Sci. China Ser. B: Chem. **35**(9), 1085–1092 (1992)
M. Li, W. Yao, Z. Li, Progress of the effect of grassland vegetation for conserving soil and water on loess plateau. Adv. Earth Sci. **20**(1), 74–80 (2005)
X.Y. Li, L.Y. Liu, S.Y. Gao, et al., Stemflow in three shrubs and its effect on soil water enhancement in semiarid loess region of China[J]. Agric. For. Meteorol. **148**(10), 1501–1507 (2008)
C. Li, D.X. Ren, G.X. Wang, H.U. Hong-Chang, L.I. Tai-Bing, G.S. Liu, Analysis of artificial precipitation interception over two meadow species on Qinghai-Tibet Plateau. Adv. Water Sci. **20**(6), 769–774 (2009)
C.J. Li, G.X. Wang, T.X. Mao, Rainfall interception by swamp meadow and alpine meadow and its seasonal distribution pattern on the Qinghai-Tibet Plateau, China. Adv. Mater. Res. **610–613**, 2675–2682 (2012)
H. Lieth, R.H. Whittaker, *Primary Productivity of the Biosphere* (Springer-Verlag, New York, 1975), p. 274
T.E. Link, M. Unsworth, D. Marks, The dynamics of rainfall interception by a seasonal temperate rainforest. Agric. For. Meteorol. **124**(3), 171–191 (2004)
X. Liu, Q. Wu, H. Zhao, The vertical interception function of forest vegetation and soil and water conservation. Res. Soil Water Conserv. **1**(3), 8–13 (1994)
H. Liu, W. Cao, X. Wang, Response of water and sediment to land use in watershed of Losses plateau. Agric. Res. Arid Areas. **28**(2), 237–242 (2010)
Y. Liu, Q. Wang, T. Yang, J. Lv, G. Zhao, Study on interception characteristics of different plants. J. Soil Water Conserv, **29**(3), (2015)
P. Llorens, F. Domingo, Rainfall partitioning by vegetation under Mediterranean conditions. A review of studies in Europe. J. Hydrol. **335**(1–2), 37–54 (2007)
P. Llorens, F. Gallart, A simplified method for forest water storage capacity measurement. J. Hydrol. **240**(1), 131–144 (2000)
D. Love, S. Uhlenbrook, G. Corzo-Perez, S. Twomlow, P. van der Zaag, Rainfall–interception–evaporation–runoff relationships in a semi-arid catchment, northern Limpopo basin, Zimbabwe. Hydrol. Sci. J. **55**(5), 687–703 (2010)
Y. Luo, Z. Ouyang, G. Yuan, D. Tang, X. Xie, Evaluation of macroscopic root water uptake models using lysimeter data. Trans. ASAE **46**(3), 625 (2003)
F.P. Lyford, H.K. Qashu, Infiltration rates as affected by desert vegetation. Water Resour. Res. **5**(6), 1373–1376 (1969)
M. Mahmoodabadi, A. Cerdà, WEPP calibration for improved predictions of interrill erosion in semi-arid to arid environments. Geoderma **204–205**(4), 75–83 (2013)
O.J. Manfroi, K. Kuraji, M. Suzuki, N. Tanaka, T. Kume, M. Nakagawa, T.O. Kumagai, T. Nakashizuka, Comparison of conventionally observed interception evaporation in a 100-m 2 subplot with that estimated in a 4-ha area of the same Bornean lowland tropical forest. J. Hydrol. **329**(1–2), 329–349 (2006)
B.A. Marsh, Measurement of length in random arrangements of lines. J. Appl. Ecol. **8**(1), 265–267 (1971)
R.B. Marston, Ground cover requirements for summer storm runoff control on aspen sites in northern Utah. J. For. **50**(4), 303–307 (1952)
J. Martinec, Snowmelt-runoff model for stream flow forecasts. Iwa Publish. **6**, 145–154 (1975)
W.J. Massman, The derivation and validation of a new model for the interception of rainfall by forests. Agric. Meteorol. **28**(3), 261–286 (1983)
C.M. Mathieu, F.O. Pieltain, Analyse physique des sols (1998)
W.C. Mayaki, I.D. Teare, L.R. Stone, Top and root growth of irrigated and nonirrigated soybeans. Crop Sci. **16**(1), 92–94 (1976)

C. Mayerhofer, G. Meißl, K. Klebinder, B. Kohl, G. Markart, Comparison of the results of a small-plot and a large-plot rainfall simulator – effects of land use and land cover on surface runoff in Alpine catchments. Catena **156**, 184–196 (2017)
J.J. Mcdonnell, M. Bonell, M.K. Stewart, A.J. Pearce, Deuterium variations in storm rainfall: implications for stream hydrograph separation. Water Resour. Res. **26**(3), 455–458 (1990)
M. McLeod, D. MacLeod, H. Daniel, The effect of degradation of phalaris+ white clover pasture on soil water regimes of a Brown Chromosol on the Northern Tablelands of NSW, Australia. Agric. Water Manag. **82**(3), 318–342 (2006)
D.W. Meals, D.C. Braun, Demonstration of methods to reduce E. coli runoff from dairy manure application sites. J. Environ. Qual. **35**(4), 1088–1100 (2006)
F.M. Melhuish, A precise technique for measurement of roots and root distribution in soils. Ann. Bot. **32**(125), 15–22 (1968)
T. Merzer, The effects of different vegetative cover on the local hydrological balance of a semi arid afforestation. Albert Katz International School for Desert Studies (2007)
L. Meyer, Rainfall simulators for soil erosion research (1994)
L.D. Meyer, D.L. Mccune, Rainfall simulator for runoff plots (1958)
D.G. Miralles, J.H. Gash, T.R.H. Holmes, R.A.M. de Jeu, A.J. Dolman, Global canopy interception from satellite observations. J. Geophys. Res. **115**(D16), D16122 (2010)
S.K. Mishra, V.P. Singh, Soil conservation service curve number (SCS-CN) methodology. Springer Science & Business Media (2013)
A. Mohammed, Rangeland condition at southern West Bank. Hebron Univ. Res. J. **2**, 42–54 (2005)
R.D. Moore, Tracing runoff sources with deuterium and oxygen-88 during spring melt in a headwater catchment, southern Laurentians, Quebec. J. Hydrol. **112**(1), 135–148 (1989)
R.R.C. Morgan, R.J. Rickson, *Slope Stabilization and Erosion Control. A Bioengineering Approach* (E & EN Spon, London, 1995)
G. Morin, V.P. Singh, D.K. Frevert, CEQUEAU hydrological model. Cequeau Hydrological Model (2002), pp. 507–576
J.P.M. Mulder, *Simulating Interception Loss Using Standard Meteorological Data* (Springer Netherlands, 1985), pp. 177–196
C. Muñoz-Robles, N. Reid, M. Tighe, S.V. Briggs, B. Wilson, Soil hydrological and erosional responses in patches and inter-patches in vegetation states in semi-arid Australia. Geoderma **160**(3), 524–534 (2011)
C.K. Mutchler, Runoff plot design and installation for soil erosion studies (1963)
C.K. Mutchler, C.E. Murphree, K.C. Mcgregor, R. Lal, Laboratory and field plots for soil erosion studies. Soil Erosion Res. Methods **9**, 36 (1988)
A. Muzylo, P. Llorens, F. Valente, J.J. Keizer, F. Domingo, J.H.C. Gash, A review of rainfall interception modelling. J. Hydrol. **370**(1), 191–206 (2009)
G. Negi, H. Rikhari, S. Garkoti, The hydrology of three high-altitude forests in Central Himalaya, India: a reconnaissance study. Hydrol. Process. **12**(2), 343–350 (1998)
T. Nehls, Y.N. Rim, G. Wessolek, Technical note on measuring run-off dynamics from pavements using a new device: the weighable tipping bucket. Hydrol. Earth Syst. Sci. **15**(15), 1379 (2011)
S.L. Neitsch, J.G. Arnold, J.R. Kiniry, J.R. Williams, K.W. King, Soil and water assessment tool theoretical documentation: version 2000, GSWRL Report 02-01, BRC Report 02-05, TR-191. College Station, Texas: Texas Water Resources Institute (2002)
J. Neris, C. Jiménez, J. Fuentes, G. Morillas, M. Tejedor, Vegetation and land-use effects on soil properties and water infiltration of Andisols in Tenerife (Canary Islands, Spain). Catena **98**(6), 55–62 (2012)
E.I. Newman, A Method of Estimating the Total Length of Root in a Sample. J. Appl. Ecol. **3**(1), 139–145 (1966)
A.R. Nordin, Eco-Engineering Practices in Malaysia. Ph.D. Thesis, University of New castle Upon Tyne, Glasgow, 1995
F.L. Ogden, B.A. Watts, Saturated area formation on nonconvergent hillslope topography with shallow soils: a numerical investigation. Water Resour. Res. **36**(7), 1795–1804 (2000)

T. Oztas, A. Koc, B. Comakli, Changes in vegetation and soil properties along a slope on overgrazed and eroded rangelands. J. Arid Environ. **55**(1), 93–100 (2003)
R.W. Pearson, Significance of rooting pattern to crop production and some problems of root research, Proc. Plant Root Environ. (1974)
H. Peng et al., Canopy interception by a spruce forest in the upper reach of Heihe River basin, Northwestern China. Hydrol. Process. **28**(4), 1734–1741 (2014)
C. Perrin, C. Michel, V. Andréassian, Improvement of a parsimonious model for streamflow simulation. J. Hydrol. **279**(1–4), 275–289 (2003)
J.R. Philip, The theory of infiltration: 1. The infiltration equation and its solution. Soil Sci. **83**(5), 345–358 (1957a)
J.R. Philip, The theory of infiltration: 4. Sorptivity and algebraic infiltration equations. Soil Sci. **84**(3), 257–264 (1957b)
M. Pidwirny, *Interception, Stemflow, Canopy Drip, and Throughfall Fundamentals of Physical Geography*, 2nd edn. (2006)
A.F. Pillsbury, R.E. Pelishek, J.F. Osborn, T.E. Szuszkiewicz, Effects of vegetation manipulation on the disposition of precipitation on chaparral-covered watersheds. J. Geophys. Res. **67**(2), 695–702 (1962)
W.T. Pinson, D.C. Yoder, J.R. Buchanan, W.C. Wright, J.B. Wilkerson, Design and evaluation of an improved flow divider for sampling runoff plots. Appl. Eng. Agric. **20**(4), 433 (2004)
O. Planchon, N. Silvera, R. Gimenez, D. Favis-Mortlock, J. Wainwright, Y.L. Bissonnais, G. Govers, An automated salt-tracing gauge for flow-velocity measurement. Earth Surf. Process. Landf. **30**(7), 833–844 (2005)
J.W. Porter, T.A. Mcmahon, A model for the simulation of streamflow data from climatic records. J. Hydrol. **13**, 297–324 (1971)
L.J. Puckett, Spatial variability and collector requirements for sampling throughfal. Can. J. For. Res. **21**(11), 1581–1588 (1991)
J.N. Quinton, G. Edwards, R. Morgan, The influence of vegetation species and plant properties on runoff and soil erosion: results from a rainfall simulation study in south east Spain. Soil Use Manag. **13**(3), 143–148 (1997)
J.C. Refshaard, B. Storm, MIKE SHE, in *Computer Models of Watershed Hydrology* (1995)
D.C. Reicosky, R.J. Millington, D.B. Peters, A comparison of three methods for estimating root length. Agron. J. **62**(4), 451–453 (1970)
K.D. Reid, B.P. Wilcox, D.D. Breshears, L. MacDonald, Runoff and erosion in a piñon–juniper woodland influence of vegetation patches. Soil Sci. Soc. Am. J. **63**(6), 1869–1879 (1999)
W.D. Reynolds, D.E. Elrick, Determination of hydraulic conductivity using a tension infiltrometer. J. Infect. Dis. **163**(4), 921–922 (1991)
M. Robinson, S.J. Grant, J.A. Hudson, Measuring rainfall to a forest canopy: an assessment of the performance of canopy level raingauges. Hydrol. Earth Syst. Sci. **8**(3), 327–333 (2004)
C.C. Romero, L. Stroosnijder, G.A. Baigorria, Interrill and rill erodibility in the northern Andean highlands. Catena **70**(2), 105–113 (2007)
M.J.M. Romkens, The soil erodibility factor: a perspective (1985)
L.A. Rossman, *Storm Water Management Model User's Manual* (2009)
V.G. Rumynin, *Surface Runoff Generation, Vertical Infiltration and Subsurface Lateral Flow* (Springer International Publishing, 2015)
J.K. Ruprecht, N.J. Schofield, Analysis of streamflow generation following deforestation in south-west Western Australia. J. Hydrol. **105**(1–2), 1–17 (1989)
A.J. Rutter, K.A. Kershaw, P.C. Robins, A.J. Morton, A predictive model of rainfall interception in forests, 1. Derivation of the model from observations in a plantation of Corsican pine. Agric. Meteorol. **9**(71), 367–384 (1971)
R. Sarkar, S. Dutta, Field investigation and modeling of rapid subsurface stormflow through preferential pathways in a vegetated hillslope of northeast India. J. Hydrol. Eng. **17**(2), 333–341 (2011)

R. Sarkar, S. Dutta, S. Panigrahy, Characterizing overland flow on a preferential infiltration dominated hillslope: case study. J. Hydrol. Eng. **13**(7), 563–569 (2008)
J.J. Schuurman, M.A.J. Goedewaagen, Methods for the examination of root systems and roots (1965)
R. Schwartz, R. Baumhardt, S. Evett, Tillage effects on soil water redistribution and bare soil evaporation throughout a season. Soil Tillage Res. **110**(2), 221–229 (2010)
M. Seeger, Uncertainty of factors determining runoff and erosion processes as quantified by rainfall simulations. Catena **71**(1), 56–67 (2007)
Z.J. Shi, Y.H. Wang, L.H. Xu, X. Wei, P.T. Yu, G. Hao, L.Y. Zhang, Hydrological functions of litter layer of typical forest types in the Liupan Mountains of Ningxia, northwestern China. J. Beijing For. Univ. **31**(1), 91–99 (2009)
M. Silgram, D.R. Jackson, A. Bailey, J. Quinton, C. Stevens, Hillslope scale surface runoff, sediment and nutrient losses associated with tramline wheelings. Earth Surf. Process. Landf. **35**(6), 699–706 (2010)
I.C. Silva, T. Okumura, Throughfall, stemflow and interception loss in a mixed white oak forest (Quercus serrata Thunb.). J. For. Res. **1**(3), 123–129 (1996)
M.J. Singer, Y. Le Bissonnais, Importance of surface sealing in the erosion of some soils from a Mediterranean climate. Geomorphology **24**(1), 79–85 (1998)
J.S. Singh, A.N. Pandey, P.C. Pathak, A hypothesis to account for the major pathway of soil loss from Himalaya. Environ. Conserv. **10**(4), 343–345 (1983)
M.V.K. Sivakumar, H.M. Taylor, R.H. Shaw, Top and root relations of field-grown soybeans. Agron. J. **69**(3), 470–473 (1977)
M.G. Sklash, R.N. Farvolden, The role of groundwater in storm runoff. J. Hydrol. **43**(1), 45–65 (1979)
M.G. Sklash, R.N. Farvolden, P. Fritz, Erratum: A conceptual model of watershed response to rainfall develop. Can. J. Earth Sci. **63**(13), 1016–1020 (1976)
K.R.J. Smettem, B.E. Clothier, Measuring unsaturated sorptivity and hydraulic conductivity using multiple disc permeameters. Eur. J. Soil Sci. **40**(3), 563–568 (1989)
A.L. Smit, J.F.C.M. Sprangers, P.W. Sablik, J. Groenwold, Automated measurement of root length with a three-dimensional high-resolution scanner and image analysis. Plant Soil **158**(1), 145–149 (1994)
R. Smith, Infiltration envelope-results from a theoretical infiltrometer. Paper presented at Transactions-American Geophysical Union, Amer Geophysical Union 2000 Florida Ave NW, Washington, DC 20009 (1971)
H.L. Smith, L.B. Leopold, Infiltration studies in the Pecos River watershed, New Mexico and Texas. Soil Sci. **53**(3), 195–204 (1942)
H.d. Snyman, C. Du Preez, Rangeland degradation in a semi-arid South Africa – II: influence on soil quality. J. Arid Environ. **60**(3), 483–507 (2005)
S. Soto-Schönherr, A. Iroumé, How much water do Chilean forests use? A review of interception losses in forest plot studies. Hydrol. Process. **30**(25), 4674–4686 (2016)
S. Strohmeier, G. Laaha, H. Holzmann, A. Klik, Magnitude and occurrence probability of soil loss: a risk analytical approach for the plot scale for two sites in Lower Austria. Land Degrad. Dev. **27**(1), 43–51 (2016)
M. Sugawara, I. Watanabe, E. Ozaki, Y. Katsuyama, Tank model programs for personal computer and the way to use (second report). Rev. Res. Disaster Prev. **113**, 1–200 (1986)
P. Suwardji, P.L. Eberbach, Seasonal changes of physical properties of an Oxic Paleustalf (Red Kandosol) after 16 years of direct drilling or conventional cultivation. Soil Tillage Res. **49**(1–2), 65–77 (1998)
K. Suzuki, Y. Kodama, T. Yamazaki, K. Kosugi, Y. Nakai, Snow accumulation on evergreen needle-leaved and deciduous broad-leaved trees. Boreal Environ. Res. **13**(5), 403–416 (2008)
Y. Tang, Research on soil erosion characteristics and vegetation cover and management factor C value of slope farmland in purple hilly region, 79 (2012)

D. Tennant, A test of a modified line intersect method of estimating root length. J. Ecol. **63**(3), 995–1001 (1975)
S. Thompson, C. Harman, P. Heine, G. Katul, Vegetation-infiltration relationships across climatic and soil type gradients. J. Geophys. Res. Biogeosci. **115**(G2), 1–12 (2010a)
S.E. Thompson, G.G. Katul, A. Porporato, Role of microtopography in rainfall-runoff partitioning: an analysis using idealized geometry. Water Resour. Res. **46**(7), W07520 (2010b)
J.H. Titus, R.S. Nowak, S.D. Smith, Soil resource heterogeneity in the Mojave Desert. J. Arid Environ. **52**(3), 269–292 (2002)
B. Torssell, J.E. Begg, C.W. Rose, G.F. Byrne, Stand morphology of Townsville lucerne (Stylosanthes humilis): seasonal growth and root development. Aust. J. Exp. Agric. **8**(34), 533–543 (1968)
P. Troch, E.V. Loon, A. Hilberts, Analytical solutions to a hillslope-storage kinematic wave equation for subsurface flow. Adv. Water Resour. **25**(6), 637–649 (2002)
A. Vacca, S. Loddo, G. Ollesch, R. Puddu, G. Serra, D. Tomasi, A. Aru, Measurement of runoff and soil erosion in three areas under different land use in Sardinia (Italy). Catena **40**(1), 69–92 (2000)
A.R. Vaezi, S.H.R. Sadeghi, H.A. Bahrami, M.H. Mahdian, Modeling the USLE K-factor for calcareous soils in northwestern Iran. Geomorphology **97**(3–4), 414–423 (2008)
T. Vogel, M. Sanda, J. Dusek, M. Dohnal, J. Votrubova, Using oxygen-18 to study the role of preferential flow in the formation of hillslope runoff. Vadose Zone J. **9**(2), 252–259 (2010)
L.X. Wang, Z.Q. Zhang, Advances in the study of ecohydrological effects from vegetation changes, World Forestry Research (6), 10 (1998)
G. Wang, Y.E.A. Zhang, *Ecohydrology in Cold Regions: Theory and Practice* (Science Press, Beijing, 2016)
X.P. Wang, Y. Cui, Y.X. Pan, X.R. Li, Z. Yu, M. Young, Effects of rainfall characteristics on infiltration and redistribution patterns in revegetation-stabilized desert ecosystems. J. Hydrol. **358**(1), 134–143 (2008)
A.W. Warrick, *Soil Water Dynamics* (Oxford University Press, New York, 2003)
F. Watanabe, Y. Kobayashi, S. Suzuki, T. Hotta, S. Takahashi Estimating the volume of surface runoff from in situ measured soil sorptivity, 沙漠研究: 日本沙漠学会誌, 22 (2012)
F. Weller, A method for studying the distribution of absorbing roots of fruit trees. Exp. Agric. **7**(4), 351–362 (1971)
C. Wels, R.J. Cornett, B.D. Lazerte, Hydrograph separation: a comparison of geochemical and isotopic tracers. J. Hydrol. **122**(1–4), 253–274 (1991)
I. White, K.M. Perroux, Estimation of unsaturated hydraulic conductivity from field sorptivity measurements. Soil Sci. Soc. Am. J. **53**(2), 324–329 (1989)
L.K. Wiersum, The relationship of the size and structural rigidity of pores to their penetration by roots. Plant Soil **9**(1), 75–85 (1957)
S.A. Wilde, G.K. Voigt, Absorption-transpiration quotient of nursery stock. J. For. **47**(8), 643–645 (1949)
G. Willgoose, H. Perera, A simple model of saturation excess runoff generation based on geomorphology, steady state soil moisture. Water Resour. Res. **37**(1), 147–156 (2001)
W.H. Wischmeier, J.V. Mannering, Relation of soil properties to its erodibility. Proc. Soil Sci. Soc. Am. **33**(1), 131–137 (1969)
L. Woodward, Infiltration-capacities of some plant-soil complexes on Utah range watershed-lands. Eos. Trans. AGU **24**(2), 468–475 (1943)
Q. Wu, Y. Liu, Ground temperature monitoring and its recent change in Qinghai–Tibet Plateau. Cold Reg. Sci. Technol. **38**(2–3), 85–92 (2004)
Q.B. Wu, B. Shi, Y.Z. Liu, Research on the interaction of permafrost and highway along Qinghai-Tiber highway. (2002)
H.Y. Xi, F. Qi, C. Zhongqiang, C. Yufei, S.I. Jianhua, S.U. Yonghong, G.U.O. Rui, Permeability characteristics of soils and their dependence on soil conditions in Ejina Oasis. J. Glaciol. Geocryol. **30**(6), 976–982 (2008)

M. Xie, H. Zhang, Y. Wang, Study on the influence of soil and water conservation measures on the speciality of run-off production and its flowing and on the starting conditions of debris flow occured by hydrodynamics. J. Beijing For. Univ. (1994)
L.H. Xu, Z.J. Shi, Y.H. Wang, W. Xiong, P.T. Yu, Canopy interception characteristics of main vegetation types in Liupan Mountains of China. Chin. J. Appl. Ecol. **21**(10), 2487–2493 (2010)
M. Yamashita, A. Ichikawa, F. Satoh, H. Shibata, Quantitative approach and problems of river hydrological simulation models. Jpn. J. Limnol. **67**(3), 267–280 (2006)
Y. Yang, Y. Mo, Z. Wang, Z. Liao, J. Deng, X. Zhang, Experimental study on anti-water erosion and shear strength of soil-root composite. J. China Agric. Univ. (1996)
W.-Y. Yao, P.-Q. Xiao, Z.-Z. Shen, C.-X. Yang, Responses of runoff process and threshold of sediment generation for different vegetation-covered plot. Shuili Xuebao (J. Hydraul. Eng.) **42**(12), 1438–1444 (2011)
L. Yi, S. Mińgan, Experimental study on influence factors of rainfall and infiltration under artificial grassland coverage. Trans. Chin. Soc. Agric. Eng. **2007**(3) (2007)
B. Yu, C.W. Rose, K.J. Coughlan, B. Fentie, Plot-scale rainfall-runoff characteristics and modeling at six sites in Australia and South East Asia. Trans. ASAE **40**(5), 1295–1303 (1997)
X. Yu, X. Zhang, J. Li, M. Zhang, Y. Xie, Effects of vegetation cover and precipitation on the process of sediment produced by erosion in a small watershed of loess region. Acta Ecol. Sin. **26**(1), 1–8 (2006)
X.X. Yu, Y.Q. Geng, L.L. Niu, Y.J. Yue, Effect of sampling scale on spatial variability of forest soil nutrient in typical watershed with Miyun Chaoguan west watershed for example. Sci. Silvae Sin. **46**(10), 162–166 (2010)
Y. Yu, W. Loiskandl, H.P. Kaul, M. Himmelbauer, W. Wei, L. Chen, G. Bodner, Estimation of runoff mitigation by morphologically different cover crop root systems. J. Hydrol. **538**, 667–676 (2016)
G.H. Zhang, B.Y. Liu, M.A. Nearing, C.H. Huang, K.L. Zhang, Soil detachment by shallow flow. Trans. ASAE Am. Soc. Agric. Eng. **45**(2), 351–357 (2002)
B. Zhang, Y.-s. Yang, H. Zepp, Effect of vegetation restoration on soil and water erosion and nutrient losses of a severely eroded clayey Plinthudult in southeastern China. Catena **57**(1), 77–90 (2004)
Z.M. Zhang, Y.U. Xin-Xiao, J.Z. Niu, L.U. Shao-Wei, W.F. Sun, X.P. Liu, Y. Zhang, Ecohydrological functions of litter on different forest stands. J. Soil Water Conserv. **19**(3), 139–143 (2005)
X. Zhang, L. Luo, W. Jing, S. Wang, R. Wang, Z. Che, Study on the distribution effect of canopy interception of Picea crassifolia forest in Qilian Mountains. J. Mt. Sc. (2007)
G.H. Zhang, R.T. Luo, Y. Cao, R.C. Shen, X.C. Zhang, Correction factor to dye-measured flow velocity under varying water and sediment discharges. J. Hydrol. **389**(1–2), 205–213 (2010a)
G.H. Zhang, M.K. Tang, X.C. Zhang, Temporal variation in soil detachment under different land uses in the Loess Plateau of China. Earth Surf. Process. Landf. **34**(9), 1302–1309 (2010b)
L. Zhang, J. Wang, Z. Bai, C. Lv, Effects of vegetation on runoff and soil erosion on reclaimed land in an opencast coal-mine dump in a loess area. Catena **128**, 44–53 (2015)
X. Zhang, W. Zhao, Y. Liu, X. Fang, Q. Feng, The relationships between grasslands and soil moisture on the Loess Plateau of China: a review. Catena **145**, 56–67 (2016)
R.J. Zhao, The Xinanjiang model applied in China. J. Hydrol. **135**(1–4), 371–381 (1992)
X.N. Zhao, F.Q. Wu, Developments and reviews of soil infiltration research. J. Northwest For. Univ. **19**(1), 42–45 (2004)
S.L. Zhao, E.C. Dorsey, S.C. Gupta, J.F. Moncrief, D.R. Huggins, Automated water sampling and flow measuring devices for runoff and subsurface drainage. J. Soil Water Conserv. **56**(4), 299–306 (2001)
M. Zhao, W. Yao, J. Wang, P. Xiao, Experimental study on influence of vegetation coverage to soil infiltration and runoff-producing of the Loess Plateau region. Soil Water Conserv. China **6**, 3 (2015)

Y. Zhou, Vegetation and erosion control: exploration on basic principle of slope engineering. Chin. J. Appl. Ecol. **11**(2), 297 (2000)
X. Zhou, Y. Wang, Q. Liu, Adaptability of four infiltration formulas on fluvo-aquic. Soil J. Irrig. Drain. **34**(8), 5 (2015)
X. Zhu, M. Ren, Formation process and regulation measures of Loess Plateau in China. Soil Water Conserv. China **119**(2), 8 (1992)
B. Zhu, Z. Li, P. Li, Z. You, Effect of grass coverage on sediment yield of rain on slope. Acta Pedol. Sin. **47**(3), 401–407 (2010)
B. Zimmermann, A. Zimmermann, R.M. Lark, H. Elsenbeer, Sampling procedures for throughfall monitoring: a simulation study. Water Resour. Res. **46**(1), W01503 (2010)